JOURNAL OF CATALYSIS 148, 348–368 (1994)

Interaction of Copper Catalysts and Si(100) for the Direct Synthesis of Methylchlorosilanes

Nicole Floquet,[1] Sefa Yilmaz, and John L. Falconer

Department of Chemical Engineering, University of Colorado, Boulder, Colorado 80309-0424

Received December 9, 1993; revised March 17, 1994

Single crystal Si(100) surfaces with a native oxide layer were reacted with methyl chloride to investigate the direct synthesis of dimethyldichlorosilane. These high purity silicon surfaces are excellent models of the reacting powders used industrially for direct synthesis. The oxide layer did not appear to inhibit reaction significantly. The copper catalyst was added to the surface by various methods, and the form of the catalyst necessary for selective reaction was determined. Reaction was carried out at atmospheric pressure in a recirculating batch reactor and the copper–silicon surfaces were characterized before and after reaction by XRD, SEM, EDS, AES, and optical microscopy. Catalysts that contained only metallic Cu or only Cu_2O did not catalyze dimethyldichlorosilane formation; both Cu and Cu_2O were needed. A mixture containing 82 wt% Cu and 18 wt% Cu_2O yielded the best selectivity (65 mol% $(CH_3)_2SiCl_2$, 33 mol% CH_3SiCl_3, and 2 mol% $(CH_3)_3SiCl$). This selectivity is comparable to those obtained in fluidized bed reactors for copper–silicon powders without promoters. Both CuCl and $Cu(HCOO)_2 \cdot 2H_2O$ catalysts were also selective for dimethyldichlorosilane formation initially, but methyldichlorosilane formed at longer reaction times. Copper formate dihydrate solution decomposed to form Cu/Cu_2O mixtures on Si(100). Because the Cu percentage was lower than 82%, however, and because formate decomposition also formed a Cu film on the surface, the selectivity was lower. Most of the catalysts reacted with silicon to form the stoichiometric alloy Cu_3Si, but some of the resulting surfaces did not react to form methylchlorosilanes. The competition between Cu_3Si formation and consumption to form methylchlorosilanes was different for the different catalysts. A correlation was seen between epitaxial growth of Cu_3Si on Si(100) and poor selectivity for dimethyldichlorosilane formation. The most selective surfaces had a randomly oriented Cu_3Si phase. The Si(100) surface reacted by forming square pyramidal pits with Si(111) sides; the pits contained Cu_3Si.

INTRODUCTION

Methylchlorosilanes (MCS) are produced industrially in fluidized bed reactors by the Rochow direct synthesis reaction of solid silicon with gaseous methyl chloride (CH_3Cl). Copper catalyzes the selective formation of dimethyldichlorosilane ($(CH_3)_2SiCl_2$, dmd) (1),

$$2\ CH_3Cl(g) + Si(s) \rightarrow (CH_3)_2SiCl_2(g),$$

which is used as a precursor for the production of linear silicone polymers (2, 3). In the absence of copper, silicon does not react readily with CH_3Cl, and when it does react, dmd is not a significant product (4). The direct synthesis reaction must attain high selectivity for the formation of dmd because the other products, particularly methyltrichlorosilane (CH_3SiCl_3, mtc), are difficult to separate from dmd. Moreover, during the subsequent processing steps to form linear silicone polymers, mtc causes chain branching.

The Rochow synthesis is sensitive to the purity of silicon, the form of the catalyst, and the presence of promoters. To better understand the surface chemical processes in this solid-catalyzed gas–solid reaction, the surface conditions need to be controlled and the surfaces need to be characterized before and after reaction. Most laboratory studies, however, have used conditions that are similar to those in industrial processing: small particles (powders) of copper catalyst and technical grade silicon are reacted in fluidized beds (1, 5, 6). A few studies have used bulk Cu–Si alloys made from high-purity materials (7–11), and one recent study used high-purity silicon in a packed bed reactor (12).

To obtain a better understanding of the Rochow synthesis of dmd, we have carried out model studies on single-crystal, semiconductor-grade Si(100) surfaces onto which copper catalysts were deposited in various forms and by various means. These surfaces are good mimics of the small particles that are used in the industrial scale reaction, but they have many advantages over the powders used in fluidized bed reactor studies. Some advantages of single crystal studies are that high purity materials are used, the flat silicon surface allows control of the reacting surface conditions, decomposition of the cata-

[1] On leave from Universite de Bourgogne, Laboratoire de Recherche sur la Reactivite des Solides, B.P. 138, 21004 Dijon Cedex, France

0021-9517/94 $6.00

lyst precursor can be observed, the crystal structure of the silicon can be controlled, the oxide thickness can be controlled, and the solid products can be analyzed. Moreover, unlike powders, which can break apart under reaction conditions, the planar silicon surface remains intact. The planar surfaces also lend themselves readily to surface analysis, and with the apparatus used in these studies, the surfaces could be analyzed by Auger electron spectroscopy (AES) without exposure to air. The planar surfaces also allow us to determine if Cu or Cu_3Si grows epitaxially on the silicon. The stoichiometric alloy, Cu_3Si, has been observed to form from copper and silicon under many conditions, and it has been implicated in the direct synthesis reaction.

After reaction for 12 to 30 hr at atmospheric pressure and 598 K, samples were removed from the reactor and analyzed by X-ray diffraction (XRD), scanning electron microscopy (SEM), energy dispersive X-ray spectroscopy (EDS), and optical microscopy. Before analysis, chemical treatments were used in some cases to remove elemental copper or copper–silicon alloys, and the Cu–Si layers were peeled off surfaces in some cases with adhesive tape. Samples were also analyzed before reaction, but after thermal treatments.

A previous study by Banholzer *et al.* (13) used single crystal silicon wafers for the direct reaction, but the wafers were located in a fluidized bed of silicon and copper catalyst particles, and thus, the products from the single crystal surfaces could not be detected. In the current study, a recirculating batch reactor was used to measure the kinetics of methylchlorosilane formation on single crystal Si(100) wafers. This allowed the direct detection of products formed from the Si(100) surfaces. Almost all silicon samples were studied without removing the native oxide layer because the silicon surface in the industrial reaction has a native oxide layer, approximately 1–2 nm thick, that is not removed before reaction.

The objective of this study is to develop a model catalyst system that yields the same product distributions obtained in fluidized bed reactors so that it can be used to study the roles of impurities, promoters, the crystal face, and other variables. The emphasis is on the identification of the form of the catalyst required for selective formation of dmd and the relation between Cu_3Si and selectivity. Thus, results from surface and bulk analysis techniques will be presented in an effort to understand the Cu–Si interaction, and detailed kinetic results will be presented in a separate paper (14). The active form of the catalyst has been reported to be the η, η', or η'' phase of Cu_3Si(1), and bulk samples of this alloy provide an active and selective surface for dmd formation (7–9). Several studies (6, 15), however, have questioned whether Cu_3Si is the active catalyst, and thus, it is of interest to characterize the Cu_3Si that forms on the Si(100) surfaces.

Copper catalysts were deposited on Si(100) surfaces by evaporation, from solution, from a slurry, and as powders. Copper was deposited as Cu, Cu_2O, CuCl, and Cu $(CHOO)_2$. The catalyst/silicon surface was then pretreated before reaction. Copper formate was used, since it had been reported previously to provide an active catalyst (16). We reported previously (17) that copper formate deposited from solution formed an active copper–silicon contact mass for reaction of single crystal silicon. The current study shows that copper formate deposited from solution decomposed to form Cu and Cu_2O, and thus, powders of elemental Cu, Cu_2O, and Cu/Cu_2O mixtures were placed directly on the surface. A mixture of Cu and Cu_2O was found necessary to create an active and selective surface, and the best selectivity (65 mol% dimethyldichlorosilane) was obtained for a mixture that contained 82 wt% elemental Cu. Another way to create an active catalyst surface was to deposit CuCl, as used previously by others (6, 12), but we observed that a surface prepared from CuCl lost much of its selectivity at longer reaction times.

Silicon single crystal wafers are shown to provide excellent surfaces to carry out model studies of the Rochow synthesis. The same methylchlorosilane products are seen as observed for powders in laboratory scale reactors, and high selectivities to dmd are observed under some conditions. In fluidized bed reactors with chemical grade silicon (99% purity) and CuCl catalyst, the selectivity for dmd was 71 mol% (5). In a fixed bed reactor with high purity silicon (99.99% purity), selectivity to dmd on freshly prepared Cu–Si mixtures was only 22 mol%, and in addition to dmd and mtc, methyldichlorosilane (CH_3SiHCl_2, mdc) was observed as a significant product (12). Zinc and tin promoters increased the selectivity for dmd formation to 91 mol% in both of these studies (5, 12). Thus, the selectivity of 65 mol% obtained in the current study shows that the single crystal wafers are an excellent model of the powders used in fluidized bed reactors.

Reacted Si(100) surfaces were observed to have square pits, as reported previously by Banholzer *et al.* (13). The structure of the pits, the form and the amount of the copper in the pits, and the concentrations of pits for various starting materials were characterized in this study. On surfaces that were not reactive for dmd formation, a Cu_3Si phase completely filled the pits and protruded from the surface. The stoichiometric alloy Cu_3Si was detected on many of the surfaces studied, but the presence of Cu_3Si did not always result in the formation of dmd. On some surfaces, Cu_3Si grew epitaxially, and for these oriented surfaces, reactivity and selectivity were poor. The best selectivity and a high reactivity were obtained for Cu_3Si that was randomly oriented on the Si(100) surface.

EXPERIMENTAL METHODS

Sample Preparation

All reactions were carried out on semiconductor-grade Si(100) wafers obtained from Virginia Semiconductor. The silicon wafers had resistivities of 0.1 Ω-cm and were *n*-type, with phosphorus concentrations of approximately 10^{17} atoms/cm^3. The silicon samples were first degreased in a 1 : 1 : 1 mixture of methanol, diethylether, and trichloroethane, and then oxidized in a boiling H_2SO_4 : H_2O_2 mixture (1 : 1) for 20 min. The samples were then rinsed in distilled water and dried in air. Ellipsometry measurements (Gaertner L116C system, 632.8 nm wavelength) showed that the resulting oxide layer was 2 ± 0.1 nm thick. Almost all experiments were run on Si(100) with a 2-nm oxide, except as noted. For those experiments where the oxide layer was removed, oxidized samples were etched in 48% HF for 10 min, rinsed in distilled H_2O, and heated four times at 1273 K in UHV for 40 s to remove carbon and oxygen, which were detected by Auger electron spectroscopy (AES).

The samples were mounted in the sample holder so they could be resistively heated, and chromel–alumel thermocouple wires were spot-welded to a thin strip of tantalum foil, which was wrapped around the sample edge. Samples were moved into the UHV chamber and characterized by AES prior to copper deposition. The methods used to deposit copper catalysts onto the silicon single crystal surfaces are described next.

Evaporated copper. Copper (Alpha Chemicals, 99.9995%) was evaporated in UHV from an alumina crucible onto the Si(100) sample, which was held at either 298 or 523 K during the deposition. The alumina crucible was located in a small evaporation chamber that was shielded by a stainless steel plate with a 1.5-cm hole. A current-regulated power supply heated the copper source, and the deposition thickness was controlled by exposure time. The deposition rate was estimated to be 10 nm/min from profilameter measurements of copper thickness. After analysis by AES, samples were transferred to the reaction chamber, without exposure to air, for reaction with CH_3Cl.

Copper formate. The copper(II) formate dihydrate (99.9% purity), from Universal Preserv-A-Chem, Inc., was dissolved in distilled water. In our previous study (17) the formate was labeled as the tetrahydrate, but subsequent XRD analysis showed it to be the dihydrate (Table 1). Solutions with concentrations of 46 and 4.3 mg $Cu(CHOO)_2 \cdot 2H_2O$/g-H_2O (solutions A and B, respectively) were used. A syringe was used to place a few drops of copper formate solution onto the Si surface, which was held at 373 K to evaporate the water. Approximately 0.5 cm^3 of solution was added over a 5-min period. After evaporation, the XRD pattern did not correspond to the dihydrate nor to any known anhydrous formate structure. The copper formate was decomposed on the silicon under UHV by ramping the sample temperature at 2 K/s to 650 K and holding at that temperature for 60 min. Carbon dioxide from formate decomposition was detected by the mass spectrometer from 430 to 650 K.

Copper formate was also deposited by placing the dry powder on the silicon surface. The formate powder was prepared by crushing particles in a mortar and pestle, and either 10 or 23 mg of formate powder was physically placed on the surface at room temperature. The dry formate powder was decomposed in UHV by the same procedure used for the formate from solution.

Powders. Samples of Cu, Cu_2O, and Cu/Cu_2O mixtures were physically placed on the silicon surface. After deposition, the silicon was resistively heated from 298 to 650 K under UHV and held at 650 K for 1 hr. Amounts used of pure powders were 63 mg of Cu powder (Aldrich, 99.999% pure, 40 μm) and 20 or 63 mg of Cu_2O powder (99.9%, Strem Chemicals Inc., 1.5 to 5 μm). Mixtures of Cu and Cu_2O powders (50/50 wt%, 82/18 wt%) were ground in a mortar and pestle, and 15 mg were placed on the surface.

TABLE 1

Structural and Morphological Properties of Cu- and Si-Containing Species

Compound	System	Space group	Parameter (nm)	JCPDS files
Si	Cubic	*FD3m*	a = 0.543	27-1402
$Cu(CHOO)_2 \cdot 2H_2O$	Monoclinic	*P2/c*	a = 0.848	16-954
			b = 0.713	
			c = 0.934	
			β = 97.00°	
Cu	Cubic	*Fm3m*	a = 0.361	4-0846
CuCl	Cubic	*F-43m*	a = 0.541	6-0344
Cu_2O	Cubic	*Pn3m*	a = 0.426	5-0667
CuO	Monoclinic	*C2/c*	a = 0.4684	5-0661
			b = 0.3425	
			c = 0.5129	
			β = 99.28°	
$Cu_5Si(\gamma)$	Cubic		a = 0.6222	4-841
$Cu_{15}Si_4(\varepsilon)$	Cubic		a = 0.9615	23-222
$Cu_3Si(\eta)$	Rhombohedric	*R-3m*	a = 0.247	Ref. (24)
			α = 109.74°	
$Cu_3Si(\eta')$	Rhombohedric	*R-3*	a = 0.472	Ref. (24)
			α = 95.72°	
$Cu_3Si(\eta'')$	Orthorhombic	*C*	a = 7.676	Ref. (24)
			b = 0.7000	
			c = 2.194	

CuCl slurry. A slurry of 170-μm particle size CuCl powder (Alpha Products, 99.999%) and hexane was placed on a Si(100) surface with an eye dropper. The silicon oxide was first removed by etching in 2% HF. After the CuCl was deposited, the sample was resistively heated to 650 K and held at this temperature for 1 h in He (83 kPa) in the reaction chamber.

Reaction Procedure

Reaction kinetics were measured in a combined UHV/atmospheric pressure system. The details of this system have been described previously (7). A bellows transfer mechanism allowed samples to be moved between UHV and the atmospheric pressure reactor without exposure to air. A Si(100) sample (1 cm^2 surface area) on which copper was deposited was held at 598 K and reacted with CH_3Cl at atmospheric pressure. A metal bellows pump recirculated the CH_3Cl over the silicon samples, and the conversion of methyl chloride was kept below 15% to minimize effects of reaction products on the kinetics. The reaction products were analyzed with a gas chromatograph equipped with a thermal conductivity detector, and product concentrations versus time were used to calculate the reaction rates. The GC column was able to separate all the methylchlorosilanes of interest, but the nonsilicon-containing products (nonsilanes) were not separated from each other. The nonsilanes are mostly methane (12, 18), and thus, methane was used for their GC calibration. Most reaction times were 12 to 20 hr, but reaction was run for more than 30 hr on some samples.

Surface and Bulk Analysis

The elemental compositions of some surfaces were measured with Auger electron spectroscopy (AES) before and after exposure to CH_3Cl. A PHI cylindrical mirror analyzer was used with a beam energy of 3 keV and a beam current of 30 μA. Surface compositions were estimated from the AES peak-to-peak amplitudes of Si (1619 eV), Cu (917 eV), Cl (180 eV), C (273 eV), and O (510 eV) transitions and published sensitivity factors (19). Shifts in the Si (LVV) peak can be used to determine the Si chemical environment.

Samples were removed from the reactor and examined by optical microscopy, scanning electron microscopy (SEM), energy dispersive X-ray spectroscopy (EDS), and X-ray diffraction (XRD) in order to identify surface species. The Nikon optical microscope could be used in reflection, transmission, and polarized light modes. Two SEM systems, Cambridge S250 MK3 and ISI SX 30, were used at beam voltages of 20 keV. In addition to obtaining a topographical view of the surface by SEM, energy dispersive X-ray spectroscopy (EDS) in the same system was used to obtain elemental copper and silicon composition maps of the wafer. Side views of some wafers were also analyzed by SEM and EDS by breaking liquid-nitrogen-cooled samples and analyzing a reacted region that was located in the break. Even though the copper–silicon surfaces are probably oxidized by exposure to air, the escape depth of emitted X-rays is sufficient that silicon and copper were readily detected by EDS. The EDS was capable of fixed spot, line scans, and mapping plots. The X-ray powder diffractometer (Scintag, Inc., PAD V) uses Cu$K\alpha$ radiation. Solid products were identified using both JCPDS computerized powder diffraction standards (20) and literature data (Table 1). The planar samples were run in the $\theta/2\theta$ mode so that only crystalline planes parallel to the Si(100) surface were detected.

Separate samples were used to characterize surfaces before and after exposure to CH_3Cl. The deposited layers on some samples were removed by adhesive tape, and on other samples elemental copper was removed by washing in 30% NH_4OH solution in an ultrasonic bath. The resulting surface was analyzed by SEM, EDS, XRD, and optical light microscopy. A few samples were further washed in a 1 : 1 NH_4OH-H_2O_2 mixture to dissolve the copper–silicon alloy, and the resulting surfaces were analyzed by SEM and EDS.

RESULTS

Evaporated Copper

No methylchlorosilanes formed on the Si surfaces on which Cu was evaporated, even after 16–17 hr exposure to CH_3Cl at 598 K. On these surfaces, CH_3Cl decomposed, nonsilanes formed, and carbon was deposited. Auger analysis indicated that the surfaces were 70–94% carbon. Results of XRD and SEM analysis for three samples follow, but many other samples, with various thicknesses of Cu, were also exposed to CH_3Cl for long times without reaction.

10-nm Cu layer deposited at 298 K. The oxide layer was removed from a Si(100) surface and a 10-nm copper layer was evaporated under UHV onto the silicon surface, which was held at 298 K. An AES analysis showed that the resulting surface was composed of 76 at.% Cu, 15 at.% Si, and a total of 9 at.% C, O, and Cl. As observed for bulk Cu_3Si (Fig. 1a), the elemental Si (LVV) peak was split into two peaks at 90 and 94 eV (Fig. 1b), indicating that copper and silicon interact at 298 K (11). The split peak does not necessarily indicate the presence of a Cu_3Si phase (21), and a silicide phase was not detected by XRD, which only detected elemental copper and silicon. Also, the relative intensities of the 90- and 94-eV peaks were different for Cu_3Si and Si with evaporated Cu, as shown in Fig. 1. The presence of silicon on the surface

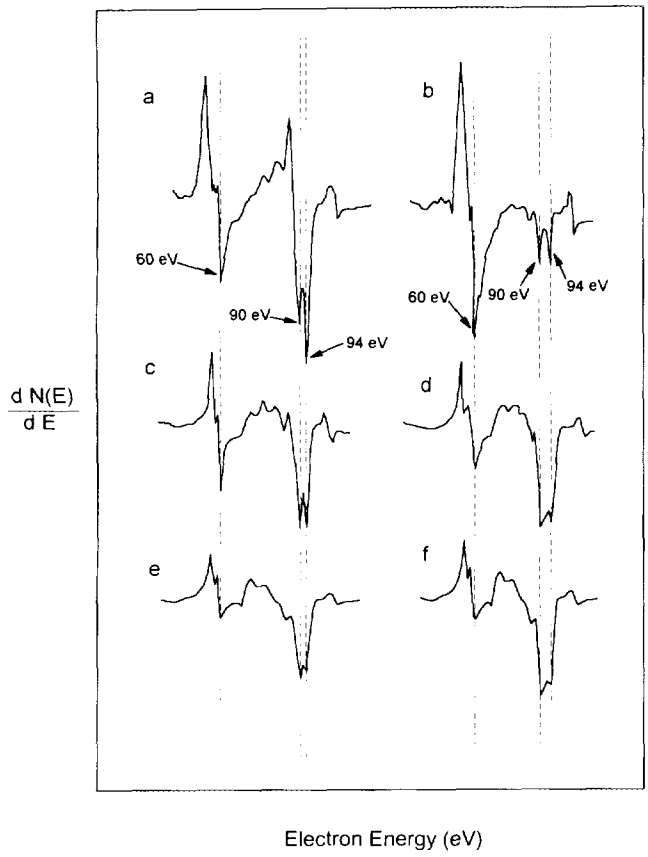

FIG. 1. Cu (60 eV) and Si (90, 94 eV) Auger peaks for (a) clean bulk Cu_3Si, (b) a 10-nm Cu layer evaporated onto clean Si(100) at 298 K, and the evaporated copper layer after heating at 600 K for (c) 4 min, (d) 23 min, (e) 48 min, (f) 124 min.

indicates that copper and silicon interdiffuse rapidly, even at 298 K (21).

Silicon surfaces with evaporated copper were heated to 598 K under UHV to determine how the surface composition changed with time at reaction temperature. As shown in Figs. 1c and d, the Cu (60 eV) intensity decreased and the Si split peak intensities increased after 4 min, apparently because silicon and copper interdiffused. The intensities of the Si split peaks started decreasing after 23 min at 598 K (Fig. 1e), and intensities of both Si and Cu peaks remained constant after 48 min (Fig. 1f). Even after heating to 598 K, no Cu–Si alloy was detected by XRD.

100-nm Cu layer deposited at 298 K. A 100-nm copper layer was evaporated under UHV onto a Si(100) surface that had a native oxide layer (2-nm oxide); the silicon was held at ~298 K during the evaporation. The copper thickness was measured by a profilameter and verified by a SEM side view photograph. The surface composition obtained from AES was 66 at.% Cu, 33 at.% Cl, and 1 at.% O, but no Si was detected. The chlorine apparently adsorbed on the Cu layer from the chamber walls. An SEM top view showed that the copper layer was smooth and uniform.

Copper and silicon phases were observed by XRD, but no copper compounds were detected (Fig. 2a). In the 2θ range analyzed (25–70°), the diffraction pattern displayed four peaks. Note that for all XRD patterns the peaks are labeled with the d-spacing in nm. The peak at 69.17° corresponds to the Si(400) d-spacing (0.1357 nm), which is the only diffraction peak expected for a Si(100) face. Its intensity is approximately 300 times greater than those of the other peaks. The peak at 33.00° characterizes a 0.2713-nm d-spacing, which is close to the Si(200) d-spacing (0.2715 nm). The Si(200) reflection is a systematic extinction of the silicon diamond structure, and it was not seen on Si(100) samples before Cu deposition. If copper diffuses into silicon, however, the structure may be modified and extinction rules can be altered so that the Si(200) peak can be observed. The shape and width of the Si(200) peak matched those of the Si(400) peak, indicating that these two peaks came from similar structures (i.e., Si bulk). Because the intensity ratio of Si(200) to Si(400) is only 0.003, most of the silicon in the X-ray detectable layer was not affected by copper.

The XRD peaks at 43.34 and 50.46° correspond to Cu(111) and Cu(200) d-spacings (0.2086 and 0.1807 nm, respectively). The copper layer was partially epitaxed since the Cu(200)/Cu(111) intensity ratio (0.17) was smaller than that in a randomly oriented Cu powder (0.46). The copper peaks halfwidths (0.135°) were broader than the silicon peaks halfwidths (0.05°). From

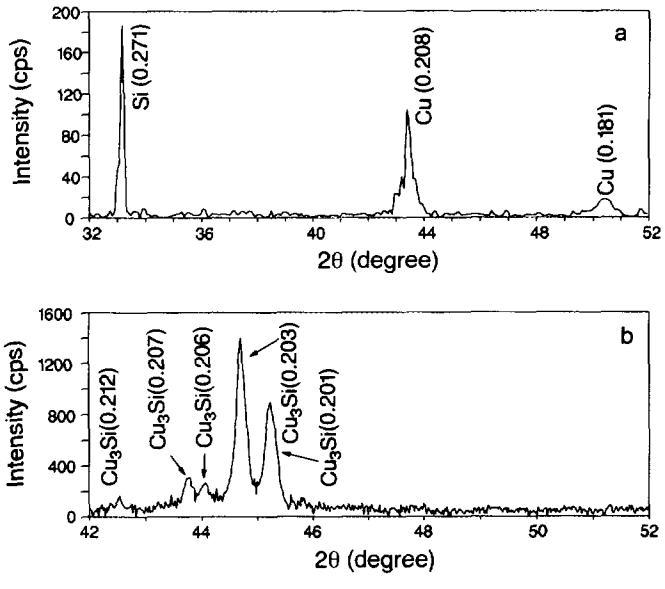

FIG. 2. XRD pattern of (a) 100-nm Cu layer evaporated at 298 K onto Si(100), (b) bulk Cu_3Si powder.

the copper peak halfwidth, the mean crystallite size of the copper particles was estimated as 0.1 μm (22).

Scanning electron micrographs showed that the surface morphology did not change after CH_3Cl exposure. An XRD analysis did not detect a Cu_3Si phase after the CH_3Cl exposure, but the Si(200) peak intensity increased and the Cu intensity decreased, apparently because additional copper and silicon interdiffused.

450-nm Cu film evaporated on Si at 523 K. A thicker copper film was evaporated onto a Si(100) surface that was held at 523 K. After deposition, the surface composition estimated by AES was 64 at.% Cu, 34 at.% Cl, and a total of 2 at.% C and O. An XRD analysis showed that both Cu and Cu_3Si phases were present (Table 2). The copper phase was characterized by Cu(111) and Cu(200) peaks, and was not oriented, since the ratio of Cu(111) to Cu(200) was similar to that of copper powder. The Cu_3Si phase was characterized by the four most intense reflections of the low temperature $Cu_3Si(\eta'')$ phase (23, 24). Table 3 displays the (*hkl*) indices of four peaks in both the rhombohedric (η') and orthorhombic (η'') crystal structures reported by Solberg (24). The XRD pattern of a Cu_3Si powder (Fig. 2b) displays five diffraction peaks in the 42° to 52° 2θ range, and the intensity ratio of the two main peaks, $Cu_3Si(0\ 2\ 9)$ at 45.16° (d = 0.2006 nm) and $Cu_3Si(38\ 0\ 0)$ at 44.65° (d = 0.2028 nm), is 0.63. The intensity ratio for these peaks from the 450-nm Cu layer on Si is 1.0, indicating that the Cu_3Si phase was partially oriented on the Si(100) face.

As shown in the SEM image (Fig. 3a), the top layer of copper was in the form of small spheres (0.2–0.6 μm diameter). The Cu_3Si phase formed a continuous skin on the Si and was also present as islands, which were observed by optical microscopy and SEM after removing metallic copper by washing in NH_4OH solution (Fig. 3b).

TABLE 2

Amplitude of XRD Peaks of CuSi Sample

	XRD peak amplitudes (cps)							
Sample	Cu (0.181)	Cu (0.208)	Cu_2O (0.246)	Cu_2O (0.213)	CuO (0.178)	Cu_3Si (0.212)	Cu_3Si (0.203)	Cu_3Si (0.201)
(a)	16	31	—	—	—	—	36	37
(b)	—	—	—	—	—	160	1,400	910
(c)	34	120	—	—	—	—	28	93
(d)	370	990	440	130	—	—	—	—
(e)	190	500	220	60	—	—	—	—
(f)	140	340	—	—	—	—	40	—
(g)	72	190	—	—	—	120	360	180
(h)	100	450	—	—	—	—	50	27
(i)	30	100	—	—	—	27	72	120
(j)	140	190	—	—	—	—	60	—
(k)	150	180	—	—	—	—	33	28
(l)	—	26	—	—	—	33	70	84
(m)	40	60	1,000	250	—	—	—	73
(n)	69	43	—	110	91	110	490	830
(o)	180	64	—	—	36	100	120	540
(p)	37	89	—	—	—	75	230	120

Note. (a) 450-nm Cu layer evaporated onto Si(100) at 523 K. (b) Bulk Cu_3Si powder. (c) Sample (a) after exposure to CH_3Cl for 16 hr at 598 K. (d) Layer formed on Si(100) by decomposition at 650 K of copper formate from solution A. (e) Particles that were brushed off sample (d). (f) Remaining surface after particles brushed off sample (d). (g) Sample after 1400 min reaction with CH_3Cl. The sample was prepared by decomposition of copper formate solution A on Si(100). (h) Brushed sample prepared from copper formate solution A after exposure to CH_3Cl for 720 min. (i) Surface prepared by decomposition of copper formate solution B on Si(100) after reaction with CH_3Cl for 600 min. (j) Surface with Cu_3Si bipyramids that was formed by decomposition of dry copper formate on Si(100). The Cu film was peeled off the surface with adhesive tape. (k) Si(100) surface on which 23 mg dry copper formate was decomposed. This surface was then exposed to CH_3Cl for 15 hr. (l) Surface on which Cu powder was deposited. The sample was held at 650 K for 1 hr and then reacted with CH_3Cl. (m) Surface on which 20 mg Cu_2O was deposited and the sample was held at 650 K for 1 hr. (n) Surface on which 63 mg Cu_2O was deposited and the surface was then reacted with CH_3Cl. Excess Cu_2O was removed before analysis. (o) Surface on which 15 mg of a Cu_2O (50 wt%) and Cu (50 wt%) mixture was deposited and then the surface was reacted with CH_3Cl. (p) Surface on which 15 mg of a Cu_2O (18 wt%) and Cu (82 wt%) mixture was deposited and then the surface was reacted with CH_3Cl.

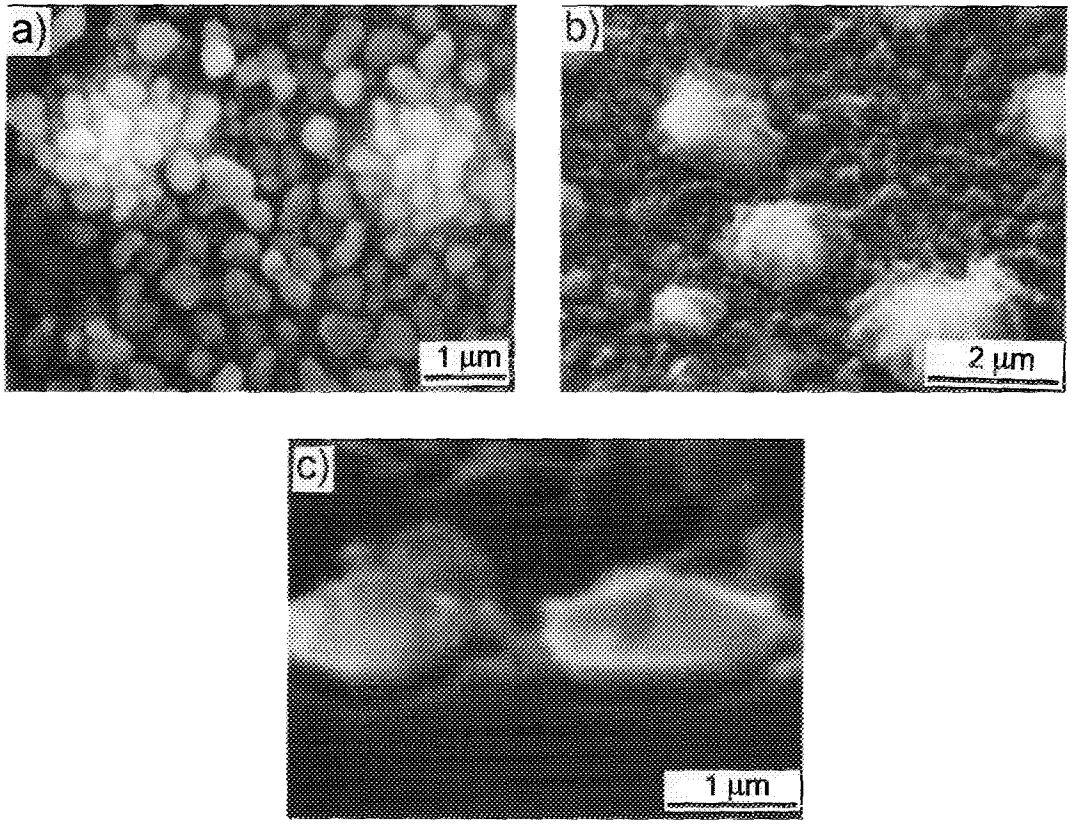

FIG. 3. SEM images for a 450-nm Cu layer evaporated onto Si(100) at 523 K: (a) small spheres in the top layer of Cu, (b) Cu_3Si skin obtained after washing the sample in NH_4OH solution, (c) side view of broken sample that shows Cu_3Si islands.

These islands were 1 to 3 μm in size, and a SEM view of a broken edge (Fig. 3c) showed that the islands were detached from their curved pits in the Si substrate.

The $Cu_3Si(0\ 2\ 9)/Cu_3Si(38\ 0\ 0)$ intensity ratio from XRD increased from 1.0 before reaction to 3.3 after CH_3Cl exposure (Table 2). The size of Cu_3Si islands remained unchanged, but SEM showed that the size of Cu particles increased after CH_3Cl exposure.

Copper(II) Formate Dihydrate

Formate solution A. The layer that formed on Si(100) after deposition and decomposition of copper formate dihydrate from solution was composed of particles and flakes on top of a mirror film. The mirror film was gold-colored and partially covered the Si surface, as observed by optical microscopy. Both Cu and Cu_2O phases were detected by XRD (Table 2). The XRD intensities of Cu_2O and Cu indicated that the formate decomposed to form approximately 33 wt% Cu_2O and 67 wt% Cu.

For some samples, the particles and flakes on top of the layer was either brushed off with a soft brush or removed by adhesive tape. The particles that were removed contained both Cu and Cu_2O according to XRD. An XRD of the remaining layer on the surface detected Cu and Cu_3Si, but no Cu_2O (Table 2). The Cu_3Si phase was characterized by a low intensity (38 0 0) peak. Since the intensity of this peak was very small, it could not be distinguished from the background. Thus, both copper particles and a copper mirror film are present, but Cu_2O was present only as particles on top of the film. As shown by the SEM images in Figs. 4a and 4b, the Cu_2O and Cu particles removed from the surface were crystallites in the shape of needles and spheres. In an optical microscope, the needles were dull yellow and the spheres were red-yellow. From XRD we estimate the percentages of Cu film, Cu particles, and Cu_2O particles as 16%, 48%, and 36%, respectively.

An SEM image of the Cu mirror film is shown in Fig. 4c. When the Cu film was removed with adhesive tape, SEM images showed that square based, bipyramidal precipitates of Cu_3Si protruded above the Si surface (Fig. 4d). The square bases of the bipyramids were aligned with the Si[011] direction, as previously reported by Weber *et al.* (23, 25). The base dimensions of these Cu_3Si bipyramids were measured as 0.8 μm from the SEM image (Fig. 4d). The number of these bipyramids was small and they yielded a low intensity Cu_3Si peak in the XRD pattern.

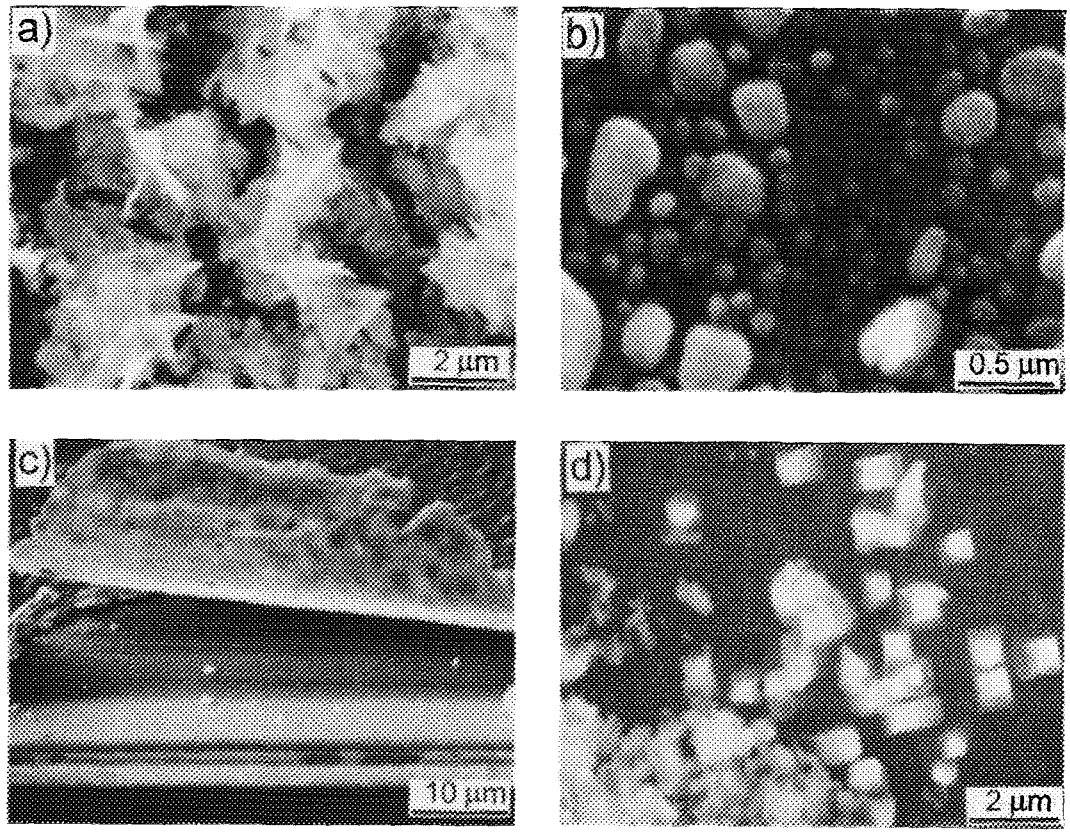

FIG. 4. SEM images of (a) the needle shape crystallites and (b) the ball shaped crystallites that were brushed off the sample formed from decomposition of copper formate solution A on Si(100). (c) the copper film slightly peeled off the Si(100) surface, (d) bipyramidal Cu_3Si precipitates after striping off the Cu film with adhesive tape.

Unbrushed surface. After decomposition of copper formate dihydrate from solution A, the surface was exposed to CH_3Cl at 598 K. Dimethyldichlorosilane ($(CH_3)_2SiCl_2$, dmd), methyltrichlorosilane (CH_3SiCl_3, mtc), methyldichlorosilane (CH_3SiHCl_2, mdc), dimethylchlorosilane ($(CH_3)_2SiHCl$, dmc) and nonsilanes formed (Fig. 5). When the reaction was stopped after 1400 min, the composition of the methylchlorosilane mixture was 43 mol% dmd, 32 mol% mtc, 22 mol% mdc, and 3 mol% dmc.

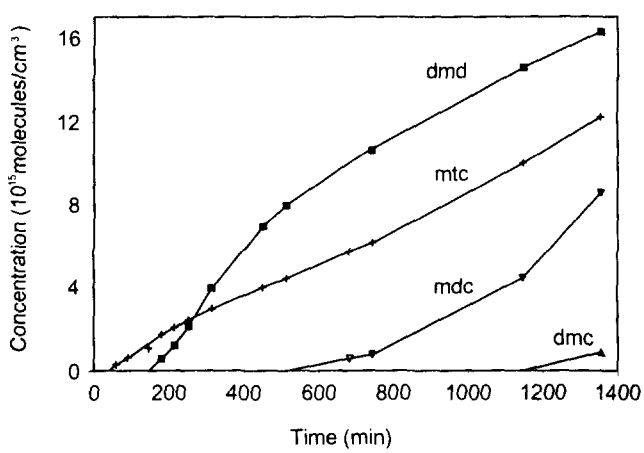

FIG. 5. Concentration versus time plot for methylchlorosilanes formed during reaction with CH_3Cl at 598 K. The sample was prepared by decomposition of copper formate solution A on Si(100).

Copper and Cu_3Si were observed by XRD on the reacted surface, but no Cu_2O was detected. The Cu intensity decreased by a factor of 5 during the reaction (Table 2). The Cu_3Si formed during reaction with CH_3Cl, and the XRD amplitude ratio of total Cu_3Si to total Cu increased from zero to 2.5 (Table 2). Either Cu or Cu_2O reacted with silicon to form Cu_3Si, since both Cu and Cu_2O amounts decreased after the reaction with CH_3Cl. Some Cu and Cu_2O may also be lost to the gas phase as CuCl.

The $Cu_3Si(0\ 2\ 9)/Cu_3Si(38\ 0\ 0)$ intensity ratio was 0.5, a value similar to that of randomly oriented, bulk Cu_3Si powder. As shown by the SEM image (Fig. 6a), discrete square based pyramidal pits (30 μm wide) formed under the Cu film, and the sides of the square bases aligned with the Si[011] direction. These pits were partially full, and were inverted pyramids, as shown in the SEM cross sectional views of a broken sample (Fig. 6b). On areas outside the film, sufficient silicon was reacted so that par-

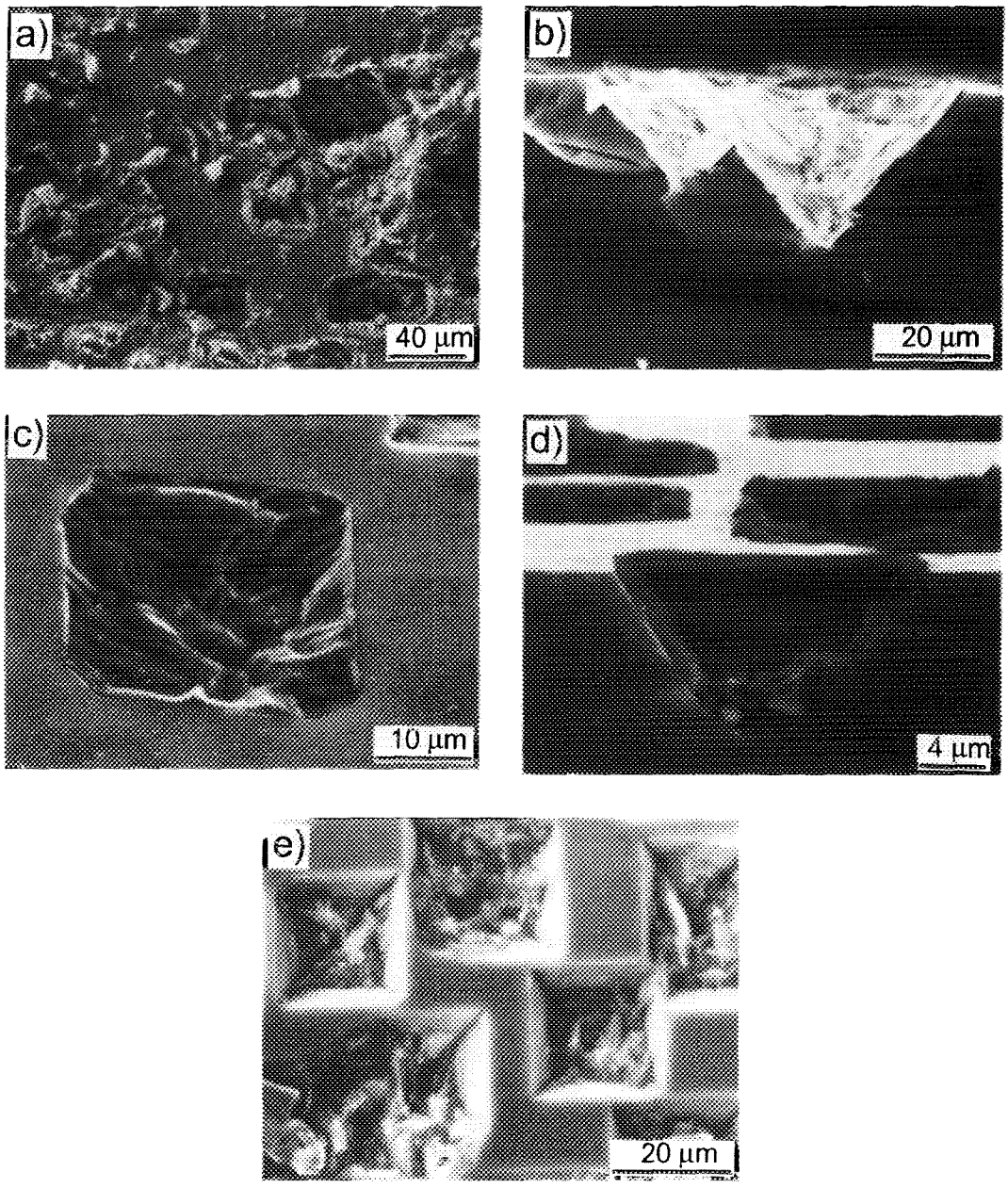

FIG. 6. SEM images of the surface formed by decomposition of copper formate solution A on Si(100) after reaction with CH_3Cl for 1400 min ((a) top view, (b) cross sectional view) and washing of the reacted sample in NH_4OH ((c) top view, and (d) cross-sectional view of the sample, which was broken parallel to Si[011] direction). The angle between the Si[011] direction and the pyramid walls is 55°, (e) further washing in a (1 : 1) mixture of H_2O_2 : NH_4OH to remove Cu_3Si.

tially full pits were connected to each other to form a continuous layer of Cu_3Si on the silicon.

The reacted surface was washed in NH_4OH, which removed metallic copper, and XRD showed that only Cu_3Si remained. Yellowish metallic-colored Cu_3Si was observed by optical microscopy as discrete square pits and pits that had grown together into a continuous layer. These pits and the layer were optically anisotropic in polarized light, indicating the presence of Cu_3Si (26). An EDS map showed that copper was present mostly in the pits and not between the pits after the sample had been washed in NH_4OH (Fig. 7). Since the XRD analysis only detected a Cu_3Si phase and optical microscopy detected Cu_3Si, the copper detected in the pits by EDS was from Cu_3Si. The Cu_3Si in the pits and in the layer of intergrown pits oxidized quickly in air and changed to a copper color overnight.

An SEM image showed that the Cu_3Si phase, which

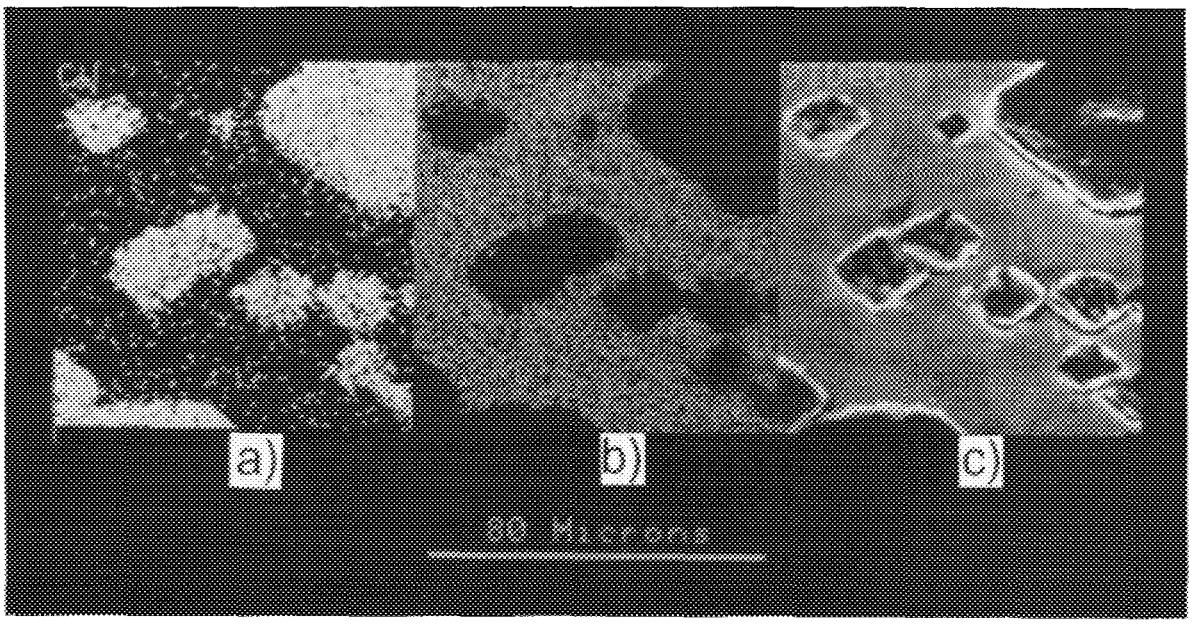

FIG. 7. An EDS map of the reacted surface showing elemental Cu (a), Si (b), and the SEM image (c) of the analyzed area. The surface was formed by decomposition of copper formate solution A on Si(100).

was identified by XRD and optical microscopy, tended to detach itself from the walls of the pits, and a thin gap developed between the Si walls and the Cu_3Si phase in the pyramidal pits (Fig. 6c). From a cross sectional view of the sample broken parallel to the Si[011] direction (Fig. 6d), the angle between Si[011] and the pyramid walls was measured as 55°. This matches the angle between the Si(100) and Si(111) planes (54.73°), indicating that the walls of these regular pyramids were {111} planes, as previously reported by Banholzer *et al.* (13). These Si{111} planes were clearly seen when a reacted sample was further washed by a H_2O_2 : NH_4OH (1 : 1) solution (Fig. 6e). This solution removed Cu_3Si and exposed the smooth {111} planes.

Before exposure to CH_3Cl, a few Cu_3Si bipyramids were present underneath the copper film, but no bipyramids were seen outside the copper film. After reaction with CH_3Cl, many new pits formed. Most of them were outside the film and were interconnected to form a rough layer. Apparently the silicon underneath the film was less reactive, despite the initial presence of Cu_3Si bipyramids, than that outside the film. Thus, the copper film hindered the reaction of silicon with CH_3Cl. The presence of pits partially full with Cu_3Si indicated that methylchlorosilanes formed from these pits; in the absence of CH_3Cl, bipyramids of Cu_3Si protruded from the surface.

Brushed surface. In one experiment, after decomposition of copper formate from solution, the surface was brushed to remove particles of Cu and Cu_2O. The remaining Cu film partially covered the surface, as shown by XRD and SEM. In contrast to the unbrushed surface, *no methylchlorosilanes formed* even after 12 hr in CH_3Cl at 598 K. The XRD intensity ratio of Cu_3Si to Cu did not change during reaction (Table 2), indicating that no additional Cu_3Si was formed during the reaction. Partially full pits with 1 μm width formed underneath the copper film, but 10 μm wide pits were observed in a few areas outside the film, indicating that the area underneath the film was less reactive. The number of pits on this surface was much smaller than that on the unbrushed one. Although no methylchlorosilanes were detected, the presence of partially full pits indicated that some silicon was removed by reaction with CH_3Cl. The product concentration may have been below the GC detection limit. These observations indicate that the Cu and Cu_2O particles are much more reactive than the Cu film in the reaction of Si with CH_3Cl.

Formate solution B. When solution B decomposed, only Cu and Cu_2O phases were detected by XRD, and the XRD intensities corresponded to 25% Cu and 75% Cu_2O. The $Cu_2O(111)$ peak halfwidth of 0.2° corresponded to a Cu_2O mean crystal size of 65 nm (22).

Methyltrichlorosilane was the only product formed from the surface deposited from solution B. After reaction, Cu and Cu_3Si phases, but not Cu_2O, were detected by XRD (Table 2). The $Cu_3Si(0\ 2\ 9)/Cu_3Si(38\ 0\ 0)$ intensity ratio was 1.8, whereas this ratio was 0.6 for a bulk Cu_3Si powder. Square-based, truncated, Cu_3Si bipyramids 7–10 μm in width were formed, as seen by SEM (Fig. 8a), and the Cu_3Si bipyramids tended to detach from

the pits. These pits were full of Cu_3Si, whereas the pits were partially full on the surface prepared from solution A. The initial percentage of Cu_2O (determined from XRD) was greater on the sample formed from solution B (Table 3).

The amount of Cu (as measured by the XRD Cu intensity) on the brushed surface from solution A was 2.5 times larger than that on the surface prepared from solution B, and copper was present as a film on the brushed surface, but only Cu and Cu_2O particles were present on

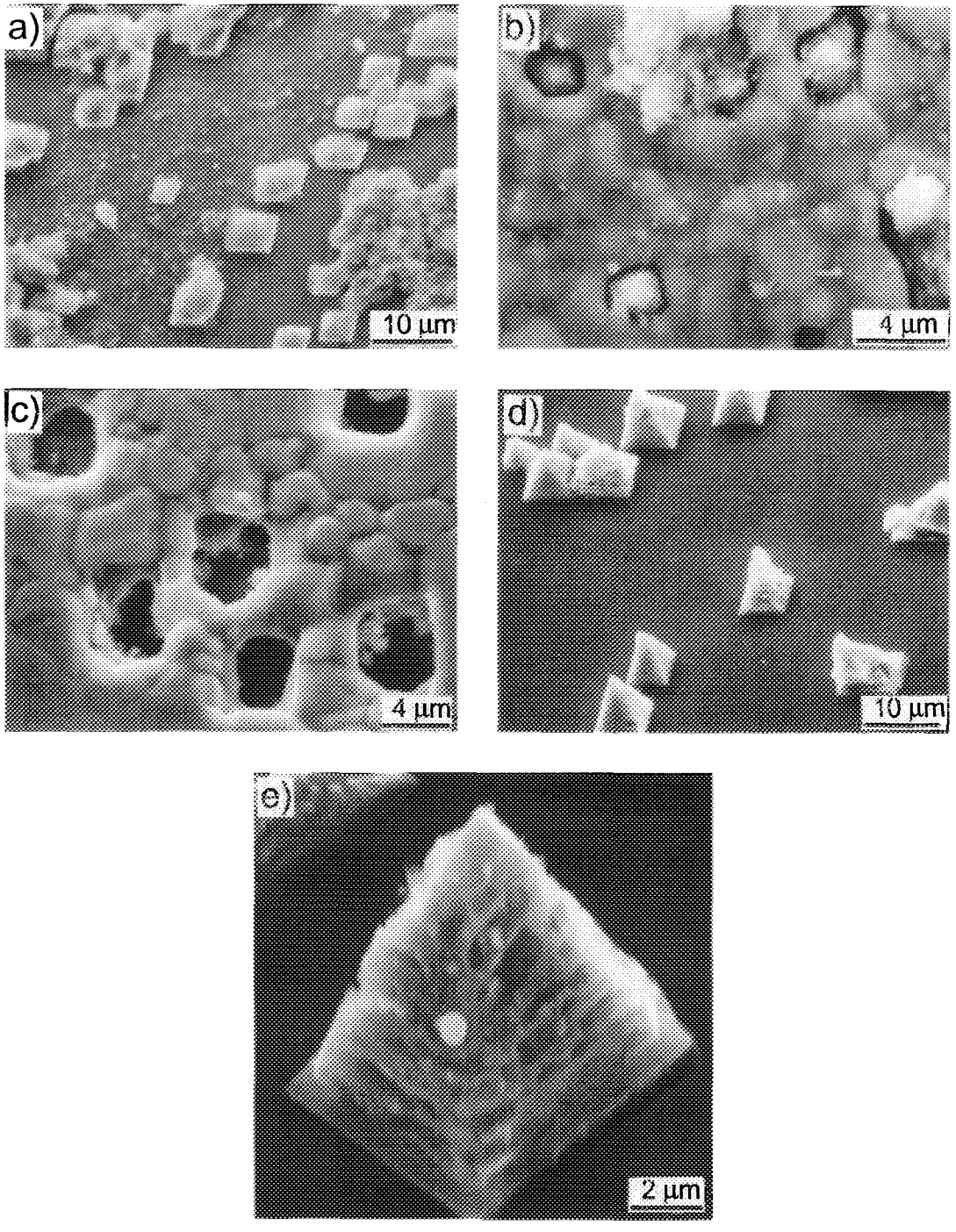

FIG. 8. SEM images of (a) a surface formed by decomposition of copper formate solution B after reaction with CH_3Cl for 600 min, (b) a surface on which dry copper formate was decomposed, (c) the reverse side of the film that was stripped from the surface deposited with dry copper formate, (d) a bipyramid formed on the surface deposited with a 33 mg dry copper formate, (e) close up view of a bipyramid in (d).

TABLE 3

Product Distributions after 800 min[a] of Reaction at 598 K

Starting catalyst	Reaction products[b] (mol%)						Cu wt%[c]
	dmd	mtc	tmc	mdc	dmc	$SiCl_4$	
Evaporated copper	—	—	—	—	—	—	100
Dry copper formate	—	—	—	—	—	—	100
Brushed formate (solution A)	—	—	—	—	—	—	100
Copper powder[d]	25	75	—	—	—	—	>95
Cu/Cu_2O powders	65	33	2	—	—	—	82
Copper formate (solution A)	59	35	—	6	—	—	66
Copper formate (solution A) at 1300 min	43	32	—	22	3	—	66
Cu/Cu_2O powders	30	70	—	—	—	—	50
Copper formate (solution B)	—	100	—	—	—	—	25
Cu_2O + evaporated Cu	—	100	—	—	—	—	1
Cu_2O powder	—	68	—	—	—	32	~0
CuCl from slurry at 200 min	53	47	—	—	—	—	NA
CuCl from slurry at 1300 min	30	24	2	37	7	—	NA

[a] Data at 800 min except as noted.

[b] dmd = dimethyldichlorosilane; mtc = methyltrichlorosilane; tmc = trimethylchlorosilane mdc = methyldichlorosilane; dmc = dimethylchlorosilane.

[c] Cu wt% (remainder is Cu_2O) before exposure to CH_3Cl.

[d] Reaction rate low, dmd formation stopped after 2 hr, and mtc formation stopped after 10 hr.

the surface prepared from solution B. Methylchlorosilanes formed on the surface made with solution B, but they did not form on the brushed sample. Thus, Cu_2O appears necessary for the formation of methylchlorosilanes on these surfaces, and Cu films are much less reactive with CH_3Cl.

Dry formate. When 23 mg of dry copper(II) formate dihydrate powder (the same amount deposited from Solution A) was physically placed on the Si surface and decomposed, a gold-colored mirror film of copper formed, and SEM showed that this film was composed of 1-μm copper spheres. X-ray diffraction only detected a Cu phase. Decomposition of dry formate did not form Cu_2O, as also reported by others (16, 27, 28). After the film was peeled off with adhesive tape, bipyramids were observed by SEM and identified as Cu_3Si by XRD. These observations are similar to those obtained from the brushed surface in that both surfaces had a copper film, small amounts of Cu_3Si in the form of bipyramids, and no Cu_2O.

When 33 mg of dry copper(II) formate dihydrate powder was placed on a Si surface and decomposed at 650 K under UHV for 2.5 hr, a thicker, gold-colored mirror of Cu covered the entire surface. The copper film was composed of grains ranging in sizes from 2 to 6 μm, and islands of Cu_3Si protruded from the surface through the copper film (Fig. 8b). After the copper film was peeled off with adhesive tape, the Si side of the film had holes where the Cu_3Si bipyramids were located, and copper grains that contacted the surface were flat (Fig. 8c). The square bases of Cu_3Si bipyramids were aligned with Si[011] direction (Fig. 8d) and the width of their square bases was 5 to 10 μm as measured by SEM. These bipyramids were formed by stacking of layers (Fig. 8e), and this layered structure of Cu_3Si was characterized by the (38 0 0) peak in the XRD pattern of the surface (Table 2).

The length of the edge of the bipyramid from the surface to its apex was approximately 13 μm, and its square base was 11 μm. These values were estimated from Fig. 8e, which is of a surface that is tilted 60°. The volume of the pyramid inside the bulk Si, and thus the amount of Si that reacted to form Cu_3Si, was calculated by assuming that the pyramid walls are (111) planes. The volume expansion from Si to Cu_3Si was calculated as 2.59 using the unit cell described by Solberg (24), and thus, the expanded volume was calculated as 812 μm^3. These values allowed the volume of the pyramid above Si to be calculated. This volume corresponds to a pyramid with an edge length of 14.6 μm, which is not far from the measured length of 13 μm.

On another sample 23 mg of dry copper formate were decomposed for 3 hr under UHV, and the sample was then exposed to CH_3Cl for 15 hr at 598 K, but *no methylchlorosilanes formed;* only nonsilanes formed. Copper plus small amounts of Cu_3Si were detected by XRD (Table 2) after exposure to CH_3Cl, and the $Cu_3Si(0\ 2\ 9)/Cu_3Si$ (38 0 0) intensity ratio was 0.8. The initial Cu_3Si bipyramids, which were 8 to 10 μm wide, were eroded after CH_3Cl exposure, and additional small pits formed that

were approximately 2 to 3 μm wide and partially full with Cu_3Si (Figs. 9a, 9b). These observations indicated that Si was removed to form methylchlorosilanes, but the rate of methylchlorosilane formation was too small to be detected by GC. The poor reactivity of this surface with CH_3Cl appears due to the absence of Cu_2O on the surface prior to CH_3Cl exposure.

Copper and Copper(I) Oxide Powders

Copper powder. When 63 mg of copper was used as the catalyst, XRD obtained after the sample was held at 650 K for 1 hr under vacuum indicated that the copper was randomly oriented, and no Cu_3Si or Cu_2O was detected. The copper particles were sintered together and most did not adhere to the surface. This surface reacted with CH_3Cl at 598 K to form mtc and small amounts of dmd (Table 3), but the formation of dmd stopped after a few hours, and mtc formation stopped after 10 hr. After reaction, Cu_3Si and Cu phases were present, and the $Cu_3Si(0\ 2\ 9)/Cu_3Si(38\ 0\ 0)$ intensity ratio was 1.2 (Table 2), whereas the ratio was 0.6 for a randomly oriented bulk Cu_3Si powder. The Cu_3Si was in the form of truncated, square-based pyramids with 1 μm widths (Figs. 9c, 9d), similar in shape to the ones formed from solution B. Because of poor contact between the copper powder and the silicon, after treatment at 650 K for 1 hr the copper powder was easily removed from the surface by brushing.

Cu_2O powder. When 20 mg Cu_2O powder was used as the catalyst, mostly Cu_2O was seen by XRD, but small amounts of Cu_3Si and Cu phases were detected (Table 2). Only the $Cu_3Si(0\ 2\ 9)$ peak was observed. Square-based pyramids, 1 to 3 μm in width and partially full with Cu_3Si, were observed and the surface was covered by copper spheres (0.15 μm) (Figs. 10a, 10b). The solid products formed after heating the Cu_2O powder on Si were not observed when Cu powder was heated on Si.

A Si wafer covered with 63 mg of Cu_2O powder formed solid products similar to those seen when 20 mg of Cu_2O powder was used. This surface reacted with CH_3Cl to produce CH_3SiCl_3 and $SiCl_4$ (Table 3). After excess Cu_2O powder was removed from the reacted surface, XRD detected Cu_2O, Cu_3Si, CuO, and Cu phases (Fig. 11a). The intensity of XRD peaks of the Cu_3Si phase increased after CH_3Cl exposure, and the $Cu_3Si(0\ 2\ 9)/Cu_3Si(38\ 0\ 0)$ intensity ratio was 1.8, indicating that the Cu_3Si phase was preferentially oriented on the Si(100) surface. The intensities of CuO and Cu phases were small. The excess powder removed from the surface contained mainly Cu_2O,

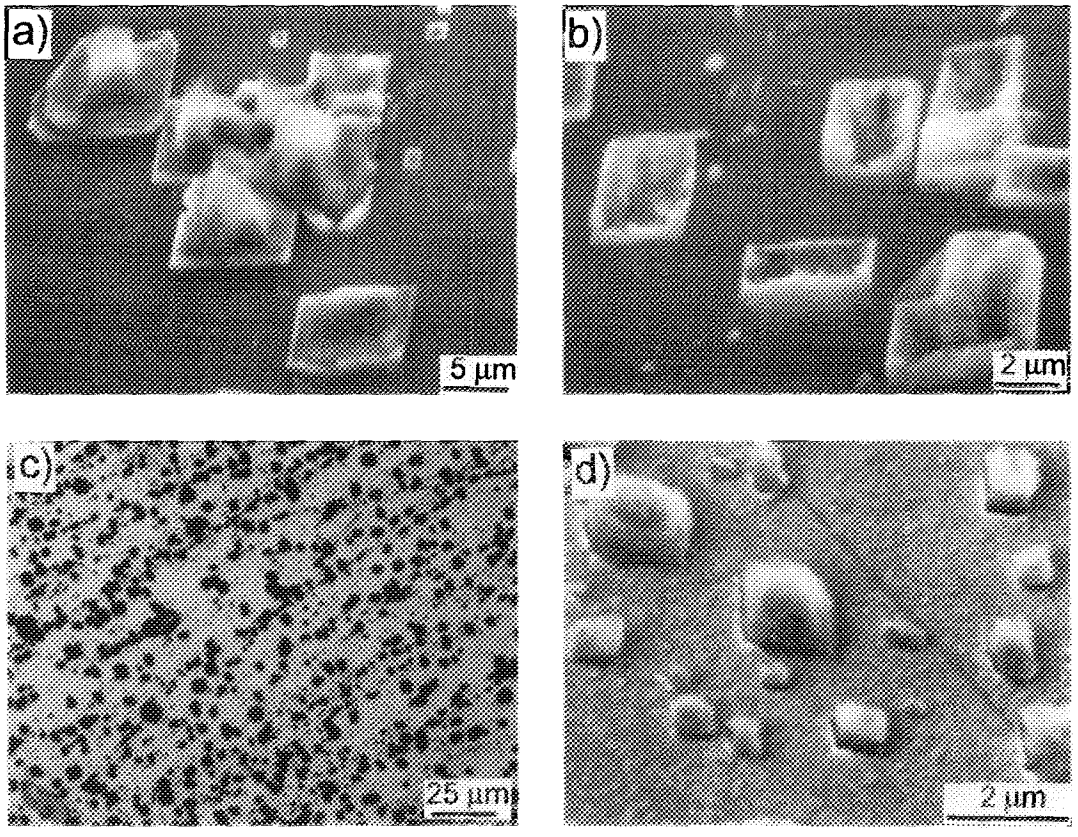

FIG. 9. SEM image of (a, b) eroded bipyramids on a Si(100) surface with 23 mg dry copper formate after exposure to CH_3Cl for 15 hr, (c, d) a surface on which Cu powder was placed and the sample was held at 650 K for 1 hr and then reacted with CH_3Cl.

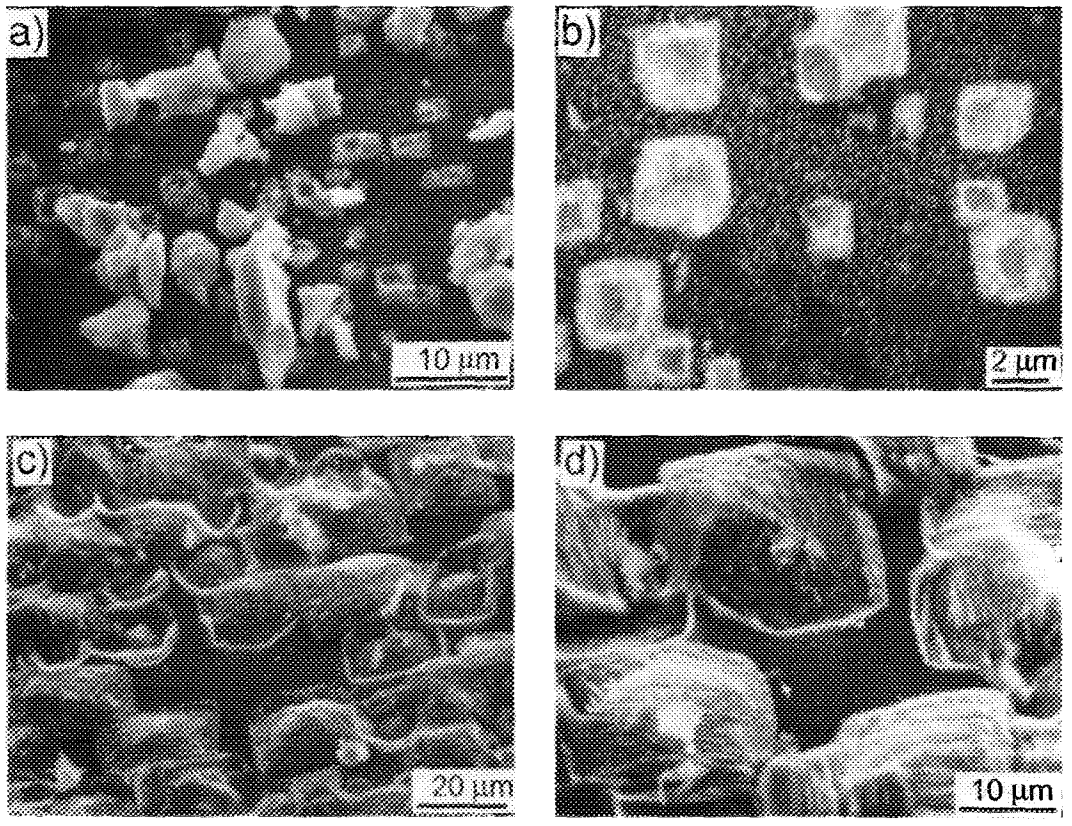

FIG. 10. SEM images of a surface on which 20 mg Cu_2O was deposited and (a, b) heated at 650 K for 1 hr. (c, d) covered with 100-nm evaporated Cu and then reacted with CH_3Cl for 18 hr.

CuCl, and a small amount of Cu. SEM and XRD analysis showed that Cu_3Si was present as a 20-μm-thick skin that was easily peeled off. Silicon layers remained attached to the Cu_3Si skin when it was removed, leaving a bare, stepped Si surface.

In another experiment, a Si surface was covered by 20 mg Cu_2O, heated under UHV at 650 K for 1 hr, and then covered with a 100-nm copper layer by evaporation. During the evaporation a large fraction of the Cu_2O particles dropped from the surface. Exposure of the surface to CH_3Cl formed mtc, but no other methylchlorosilanes formed. After reaction, Cu_2O, Cu_3Si, CuO, and Cu phases were detected by XRD. The $Cu_3Si(0\ 2\ 9)/Cu_3Si(38\ 0\ 0)$ intensity ratio peaks was 3.0 due to preferential orientation of Cu_3Si on the Si(100) surface. As shown by SEM images (Figs. 10c, 10d), the Cu_3Si phase filled the oriented pyramidal pits, and a thick Cu_3Si layer was not observed. Moreover, the Cu_3Si phase had a stacking feature aligned with the edge of the square base. This feature may be related to the preferential orientation revealed by XRD. The width of these Cu_3Si pyramids was 15 μm. This surface had less Cu_2O than the surface on which 63 mg Cu_2O was deposited, and this surface formed only mtc as opposed to mtc and $SiCl_4$. Moreover, the 100-nm evaporated Cu layer (45 μg Cu) did not seem to affect the reactivity and selectivity of the surface.

Mixtures of Cu_2O and Cu Powder. For a 50 wt% Cu_2O/50 wt% Cu mixture (15 mg) as the starting catalyst, the surface reacted with CH_3Cl at 598 K to form 30 mol% dmd and 70 mol% mtc. An XRD analysis of the reacted surface indicated that Cu_3Si, Cu_2O, CuO, and Cu phases were present. The $Cu_3Si(0\ 2\ 9)/Cu_3Si(38\ 0\ 0)$ intensity ratio was 5.6 (Fig. 11b) indicating that the Cu_3Si phase was highly oriented. Square based Cu_3Si pyramids observed by SEM ranged in sizes from 6 to 10 μm.

A 15-mg mixture of powders containing 18 wt% Cu_2O and 82 wt% Cu was a more effective catalyst. Reaction at 598 K formed a product mixture that was 65 mol% dmd, 33 mol% mtc, and 2 mol% tmc ($(CH_3)_3SiCl$). As shown in Fig. 12, reaction continued for 18 hr with high selectivity and good rate. When this experiment was repeated on a fresh sample, the product distribution was very similar (67 mol% dmd, 31 mol% mtc, and 2 mol% tmc).

An XRD analysis of the reacted surface showed Cu_3Si, Cu, Cu_2O, and CuO phases, but the intensities were low for Cu_2O and CuO (Fig. 11c). The XRD intensity ratios of Cu to Cu_2O and Cu_3Si to Cu were about 6 and 3, respec-

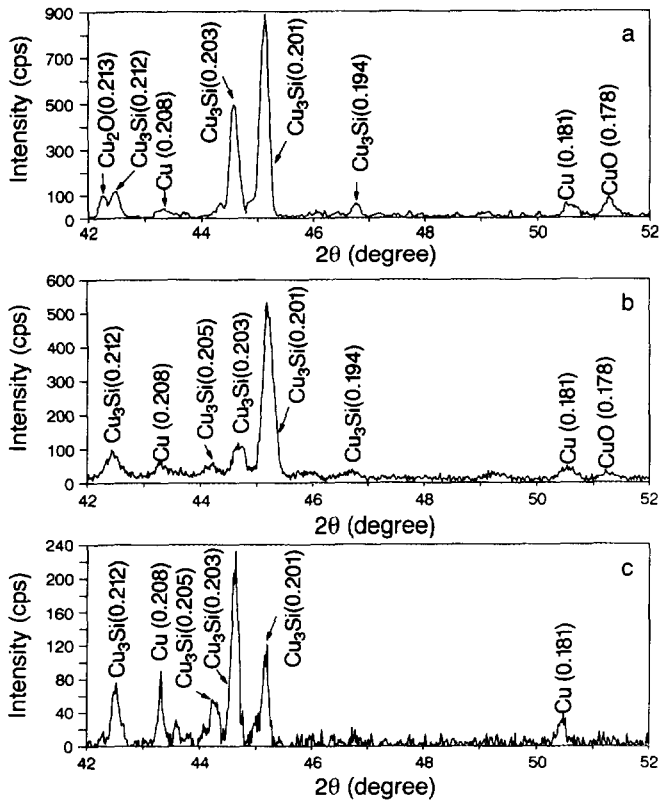

FIG. 11. XRD pattern of (a) a surface on which 63 mg Cu_2O was deposited and the surface was then reacted with CH_3Cl. Excess Cu_2O was removed before analysis, (b) surface on which 15 mg of a Cu_2O (50 wt%) and Cu (50 wt%) mixture was deposited and then it was reacted with CH_3Cl, (c) surface on which 15 mg of a Cu_2O (18 wt%) and Cu (82 wt%) mixture was deposited and then it was reacted with CH_3Cl.

tively. The $Cu_3Si(0\ 2\ 9)/Cu_3Si(38\ 0\ 0)$ intensity ratio was 0.52, which indicates that Cu_3Si was randomly oriented on the Si(100). Interconnected and discrete square-based pyramidal pits were observed by SEM (Fig. 13a,b). These pits ranged from 4 to 10 μm in width and were partially full of Cu_3Si. These results were similar to those from solution A in that both surfaces had a randomly oriented Cu_3Si phase that partially filled the pits. No mdc formed from the surfaces prepared from a mixture of Cu_2O and Cu powders. In contrast, when copper formate was deposited from solution, mdc formed in high yields after long reaction times.

CuCl Powder

Silicon and CuCl reacted at 650 K in He flow to form $SiCl_4$. After 1 hr at 650 K, the surface composition was estimated by AES as 72 at.% Cu, 10 at.% Si, 12 at.% O, 5 at.% C, and 1 at.% Cl. The Si(LVV) peak was split into two peaks at 90 and 94 eV due to Si interaction with Cu.

This surface reacted with CH_3Cl at 598 K to form dmd, mtc, mdc, dmc ($(CH_3)_2SiHCl$), and tmc. Initially, the product mix contained 53 mol% dmd and 47 mol% mtc, but selectivity for dmd formation decreased continuously after the other products started forming (Table 3). SEM showed that the reacted surface was rough and no individual pits were recognized because all the pits were interconnected. XRD detected Cu, CuCl, and Cu_3Si phases on the reacted surface. The CuCl phase was characterized by CuCl(111) and CuCl(200) peaks.

DISCUSSION

We have shown that the interaction between copper-containing catalysts and silicon surfaces depends dramatically on the form of the catalyst precursor. The composition of the catalyst, its structure, and its ability to selectively catalyze the direct synthesis of methylchlorosilanes all depend on the initial form of the catalyst. This study has characterized the various structures that form; most of the starting forms of copper were not good catalysts. In particular, copper metal alone did not catalyze the formation of dimethyldichlorosilane (dmd), independent of how it was placed on the surface.

With an appropriate catalyst (a Cu/Cu_2O dry powder mixture), high purity silicon (99.9996%) readily reacts with CH_3Cl to selectively form dmd. A selectivity of 65 mol% for dmd formation was obtained in the absence of zinc and tin promoters. Thus, a Si(100) surface with a native oxide layer appears to be a good model surface for the direct synthesis reaction on high surface area silicon particles in fluidized bed reactors. The Si(100) surfaces have the advantage, however, that the reacted surfaces can be much better characterized and the conditions of the initial surface can be better controlled. In addition to selectively forming dmd, the Si(100) surfaces showed the same overall product distribution observed for high surface area silicon powders, and Si(100) surfaces reacted

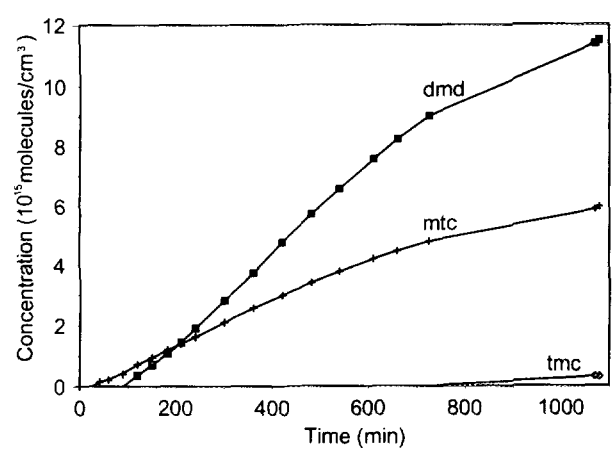

FIG. 12. Concentration versus time plot of methylchlorosilanes formed during reaction of CH_3Cl with a Si(100) surface on which 15 mg of a Cu_2O (18 wt%) and Cu (82 wt%) mixture was deposited.

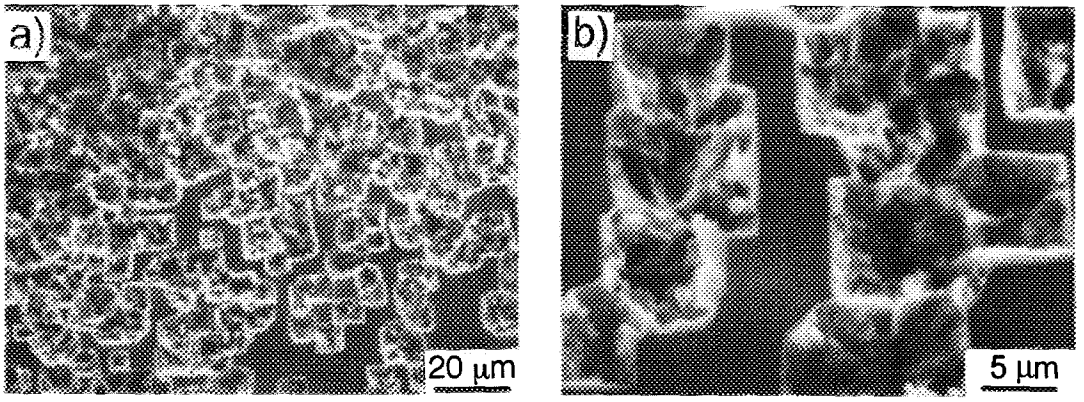

FIG. 13. (a, b) SEM images of a reacted surface after 18 hr in CH_3Cl. The catalyst was 15 mg of a 82 wt% Cu/18 wt% Cu_2O mixture that was placed on the Si(100) surface.

for long times at relatively constant rates. Methyltrichlorosilane (mtc) was the product with the next highest concentration, and trimethylchlorosilane (tmc) was a minor product. No other products were observed. Thus, single crystal silicon should be useful as a model surface to understand the roles of impurities and promoters in the direct synthesis reaction.

Selectivity and Catalyst Composition (Cu/Cu_2O)

The most important variable for obtaining high selectivity for the direct synthesis reaction on Si(100) is the composition of the catalyst. Elemental Cu and Cu_2O are either not active or not selective catalysts when used by themselves, but when physically mixed together they form a highly effective catalyst, as shown in Table 3. The highest selectivity was obtained for a mixture of Cu and Cu_2O powders that contained 82 wt% Cu. Other mixtures of Cu and Cu_2O catalyzed formation of dmd less selectively. When pure Cu_2O powder was used, only mtc formed. Similarly, when a low concentration solution of copper formate was used (solution B), mostly Cu_2O formed upon formate decomposition, and this surface only formed mtc. When a high-concentration solution of copper formate was used (solution A), both Cu and Cu_2O formed upon the formate decomposition, and thus, the resulting surface formed dmd with good selectivity. At longer times, however, mdc became a significant product when copper formate solution was used. The experiment with a brushed sample confirmed the need for both Cu and Cu_2O in the catalyst. When the particles that formed from formate decomposition were brushed off the surface, all the Cu_2O was removed, and *no methylchlorosilanes formed* on the resulting surface that contained only Cu as the catalyst.

Figure 14 shows a plot of product distribution, after 800 min of reaction, versus percentage of Cu in the catalyst at the start of the reaction. At both low and high Cu percentages, the selectivity drops off to zero. The behavior appears to be the same at 800 min whether dry powders or copper formate were used. The maximum in dmd selectivity for 82% Cu is a shallow maximum, and a range of concentrations appear to be effective for good dmd selectivity. The rates for dmd formation are similar (3.4 and 4.7 $\times$ 10^{15} molecules/cm^2/min) for the two catalysts with the best selectivity.

Elemental Cu did not catalyze formation of any methylchlorosilanes when Cu was evaporated onto Si(100). For a copper powder the selectivity to dmd was 25%. The reaction rates were low, however, for Cu powder and reaction stopped after 10 hr. Moreover, the Cu powder was not reduced and thus probably contained Cu_2O, which is present as a skin on Cu particles (29, 30). Thus, these catalysts were assumed to contain 5% Cu_2O. When dry copper formate decomposed, only elemental Cu

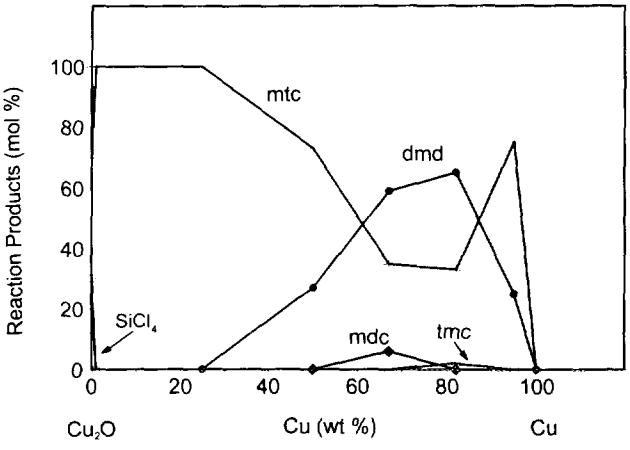

FIG. 14. Plot of product percentage at 800 min reaction time versus weight percent of Cu in the catalyst at the start of reaction. The remainder of the catalyst is Cu_2O. The catalysts were obtained by various methods. The product percentages were those measured after 800 min of reaction.

formed, and the resulting surface did not react to form methylchlorosilanes. The Cu formed from dry copper formate was in the form of a film, and this may affect reactivity.

Catalysts other than Cu/Cu_2O

High selectivity, relatively constant rates, and the absence of byproducts such as mdc were obtained for Cu/Cu_2O mixtures on high purity Si(100). Clearly, other catalysts can be used, and copper formate is effective for initiating the reaction, but it also catalyzes formation of mdc at longer times on Si(100). Likewise, CuCl deposited from a hexane slurry was effective, but mdc eventually became the dominant product for CuCl-catalyzed reaction. Methyldichlorosilane was also a major product in the study by Gaspar-Galvin *et al.* (12). They used a CuCl catalyst and high purity silicon (99.99%). Banholzer *et al.* (13) used a fluidized bed reactor that contained both high-purity, single crystal silicon wafers and technical grade silicon powder (98.5%). The much higher surface area of the silicon powder prevented detection of products from the silicon wafers, however. Since they used a CuCl catalyst deposited from a slurry, it is likely that their silicon wafers also formed mdc. Fluidized bed reactors with chemical grade silicon (99%), which is significantly lower purity than our Si(100), had good selectivity with CuCl catalysts, but the significant concentration of impurities may be important (6, 13, 31).

The best selectivity measured for dmd formation on our Si(100) surfaces was 65%, which is similar to that measured in a fluidized bed reactor with chemical grade Si (71% dmd selectivity (5)). A fixed bed reactor with high purity silicon (99.99% Si) only had a dmd selectivity of 22% because mdc was a significant product, but an aged contact mass in the same reactor had a higher selectivity (45%). The rates are significantly different for these studies, but so are the catalyst loadings, and in addition CuCl was used in the high surface area studies. The total rate of methylchlorosilane formation on Si(100) for our Cu/Cu_2O catalyst was 1.7×10^{16} molecules/cm^2/min. For the study of Gaspar-Galvin et al. (12), it was 0.2×10^{16} molecules/cm^2/min and for the study of Ward et al. (5), it was 20×10^{16} molecules/cm^2/min. These rates are based on the silicon surface areas reported for the powdered silicon.

In large scale reactors, mixtures of Cu and copper oxides are used instead of CuCl (32). The industrial reaction often uses a cement copper, which is a mixture of Cu and copper oxides. Lewis *et al.* (16) reported a typical composition of cement copper as 10.7 wt% Cu, 43.2 wt% Cu_2O, and 42.3 wt% CuO. The total metallic copper content varies from 10–20 wt%, the Cu_2O content from 30–40 wt%, and the CuO content from 45–60 wt% (33). This is quite different from what we find is best for our catalysts, but the Zn and Sn promoters and the silicon impurities can dramatically affect the surface interactions.

Cu_3Si Orientation

In the 42–52° 2θ range of the XRD pattern, the two largest peaks from the $Cu_3Si(\eta'')$ phase are

Cu_3Si(38 0 0) and Cu_3Si(19 3 0) at $d = 0.2028$ nm ($2\theta = 44.65°$)

Cu_3Si(0 2 9) and Cu_3Si(19 1 9) at $d = 0.2006$ nm ($2\theta = 45.16°$).

There is no agreement on the attribution of XRD peaks for Cu_3Si (24, 34–36). We choose the (*hkl*) indices reported by Solberg ((24), Table 3). The structure of the $Cu_3Si(\eta'')$ phase described by Solberg was a 2-D, long-period superlattice of the ordered $Cu_3Si(\eta')$ phase. For a Cu_3Si powder, we observed a Cu_3Si(0 2 9)/Cu_3Si(38 0 0) intensity ratio of 0.63, but for copper deposited on silicon, the intensity ratio depended on the method of deposition. For example, only the Cu_3Si peak at $d = 0.2028$ nm was observed when dry copper formate was the starting catalyst (Table 4), and SEM showed that Cu_3Si was present as bipyramids, layered parallel to the Si(100) surface (Fig. 8e). In contrast, only the Cu_3Si peak at $d = 0.2006$ nm was observed for Cu_3Si formed from Cu_2O powder on Si(100), and the pyramidal pits were not layered parallel to the Si(100) surface. After reaction, the Cu_3Si(0 2 9)/Cu_3Si(38 0 0) ratio was 3, and the SEM showed layers in the Cu_3Si pyramids that were perpendicular to the Si(100) face. Thus, the Cu_3Si growth mechanisms are different for Cu_2O powder and Cu that formed by decomposition of dry copper formate.

Previous studies also found that preferential orientations of Cu_3Si on silicon depended on the method of Cu_3Si formation and the nature of the silicon surface. Echigoya *et al.* (37) obtained their Cu_3Si by evaporating 1 μm of Cu onto Si(100) and heating the sample in Ar for 30 min at 523 K. They used the diffraction patterns and the lattice fringe images in TEM to obtain the orientation

TABLE 4

d-Spacings and Corresponding (*hkl*) Planes of η' and η'' Phases of Cu_3Si

d_{hkl} (nm)	(*hkl*)′	(*hkl*)″
0.203	($\bar{2}$11)	(38 0 0); (19 3 0)
0.201	(210)	(0 2 9); (19 1 9)
0.143	(31$\bar{1}$)	(38 2 9); (0 4 9)
0.117	(3$\bar{3}$0)	(57 3 0), (0 6 0)
	(32$\bar{2}$)	(19 5 9); (38 4 9);
	(40$\bar{1}$)	(57 1 9)

relationships between Si and $Cu_3Si(\eta'')$. They observed that the $(010)\eta''$ plane was parallel to the Si(100) plane, $(100)\eta''$ was parallel to Si(011), and $(001)\eta''$ was parallel to Si(01$\bar{1}$). Chang (38) obtained Cu_3Si on Si(100) by heating 1 μm of evaporated Cu in N_2/H_2 for 1 h at 473 K, and they only observed the diffraction peak at d = 0.2028 nm in XRD patterns. Setton *et al.* (39) reported from XRD analysis the same orientation of Cu_3Si, which was obtained by heating a 50-nm Cu layer, evaporated on Si(100), at 473 K. We observed similar XRD patterns of Cu_3Si bipyramids grown on Si(100) when dry copper formate was the starting catalyst. In the $Cu_3Si(\eta'')$ structure, the $(19\ 3\ 0)\eta''$ planes at d = 0.2028 nm are tilted 30° from the $(010)\eta''$ planes. Thus our results agree with those obtained by Chang (38) and Setton *et al.* (39); the orientation reported by Echigoya *et al.* (37) is tilted 30° from these other observations.

Harper *et al.* (40) obtained Cu_3Si from 100 nm of Cu deposited onto Si(100) by dc magnetron sputtering, which heats the wafer above 423 K. The Cu_3Si phase formed as Cu deposited, and XTEM shows particles of Cu_3Si epitaxially oriented relative to the Si(100). The epitaxial orientation was not precisely determined. We also obtained Cu_3Si that was preferentially oriented during deposition when we evaporated Cu onto Si(100) at 523 K.

Studies by TEM and XRD also found preferential orientation of Cu_3Si on Si(111) (24, 41). Solberg (24) evaporated 30 nm of Cu onto Si(111) and heated the sample for 20 min at 1173 K. He reported that the $(010)\eta''$ plane was parallel to the Si($\bar{1}01$) plane, the $(100)\eta''$ plane was parallel to Si($\bar{1}2\bar{1}$), and the $(001)\eta''$ plane was parallel to Si($1\bar{1}1$). An orientation with the $(001)\eta''$ plane parallel to Si($1\bar{1}1$) was observed for samples prepared by CVD of CuCl/Ar mixtures at 573 K (41). At lower temperatures, Cu_3Si particles were not as well oriented and additional XRD peaks (Cu_3Si(38 0 0) and Cu_3Si(0 2 9)) were observed. In our study, Cu_3Si particles grew on Si(100) wafers from pyramidal pits with Si(111) walls. Our XRD analysis only detected Cu_3Si planes parallel to the Si(100) surfaces. If the orientation of Cu_3Si on Si(111) walls is the one reported by Solberg (24) and Lampe *et al.* (41), the orientations $(0\ 2\ 9)\eta''$ and $(19\ 1\ 19)\eta''$, which are both at d = 0.2006 nm, are tilted 20° relative to Si(100). The 0.2006 nm diffraction peak was observed for Cu_3Si formed from Cu_2O powder on Si(100).

The preferential orientations observed in our studies are thus expected based on these previous studies. Moreover, the different orientations obtained for different preparation methods are also expected. These results are related to the growth mechanism of Cu_3Si, for which Cu vacancies play an essential part (24). The lack of agreement in the structural determination of Cu_3Si indicates that the structure of the $Cu_3Si(\eta'')$ phase is not unique, but consists of an ordered $Cu_3Si(\eta')$ phase with copper vacancies. These structural differences for Cu_3Si, which were obtained for different preparation methods, may be responsible for the differences in reactivity and selectivity observed in our studies.

Selectivity and Cu_3Si Orientation

Table 3 shows that there is a good correlation between the percentage of Cu in the Cu/Cu_2O catalyst and the selectivity for dmd formation. As discussed in the previous section, the orientation of the Cu_3Si phase appears to correlate with the type of catalyst. Thus, it appears that when the Cu_3Si phase is oriented on Si(100) at the completion of reaction, the Cu/Si combination is not active for selective formation of dmd. Moreover, the oriented Cu_3Si phase is observed as bipyramids on the surface after reaction, indicating that this Cu_3Si phase did not react with CH_3Cl. In contrast, when the Cu_3Si(0 2 9)/Cu_3Si(38 0 0) XRD intensity ratio is similar to that measured for Cu_3Si powder, dmd is a major product of reaction. On Si(100) surfaces that form dmd, the pits are only partially full, apparently because the Cu_3Si phase in the pits reacted with CH_3Cl. The XRD, EDS, optical microscopy, and $NH_4OH:H_2O_2$ washing experiments all indicated that the phase in the partially full pits is Cu_3Si. That is, higher selectivity is obtained when Cu_3Si is not epitaxially grown on silicon.

The higher selectivity for surfaces for which Cu_3Si is randomly oriented on Si(100) is consistent with results on bulk Cu_3Si. The initial selectivities for dmd formation on Cu_3Si bulk samples, which were polycrystalline and did not have any preferential orientation, were high (7) and the secondary products were those observed in fluidized bed reactors. As reaction proceeded and unalloyed Si was not available to replace the reacted silicon; however, selectivity and activity decreased on these bulk samples. On Si(100), fresh silicon was available to replenish the Cu_3Si as reaction proceeded.

The orientation of Cu_3Si may be a controlling factor in the selective formation of dmd, but other factors are important, such as the concentrations of copper vacancies and defects in the $Cu_3Si(\eta'')$ phase. Determining exact structures is difficult because of the Cu vacancy structure of Cu_3Si. The resulting Cu_3Si structure is highly dependent on how it is formed, and therefore its reactivity depends on how it is formed. Thus, bulk Cu_3Si samples, obtained by melting Cu and Si at 1473 K, had good dmd selectivity at short reaction times (7, 8), but Cu_3Si particles formed by evaporating Cu onto Si(100) at 523 K were unreactive. The reactivity of Cu_3Si with CH_3Cl depended on its copper vacancies structure and the size of its particles; both factors are related to the mechanism of Cu_3Si formation.

Role of Cu_3Si

Although Cu_3Si was observed on all samples that produced methylchlorosilanes, the amount of Cu_3Si present after reaction did not correlate with the reaction rate. For example, when 63 mg Cu_2O was used as the catalyst, a large amount of XRD-detectable Cu_3Si formed, but the rate of methylchlorosilane formation was not high and no dmd formed. When 15 mg of a Cu/Cu_2O powder mixture was used, less Cu_3Si was observed after reaction, but more methylchlorosilanes formed and dmd was one of the main products.

Since the size of the pits increases as reaction proceeds, and the surfaces with good selectivity and activity have pits that are partially full with Cu_3Si, the amount of Cu_3Si appears to increase during reaction. For almost all samples, more X-ray detectable Cu_3Si was present after reaction. The surface processes that take place during reaction might include a competition between Cu_3Si formation and reaction,

$$Cu + Si \rightarrow Cu_3Si \quad [1]$$

$$Cu_3Si + CH_3Cl \rightarrow \text{methylchlorosilanes} + Cu. \quad [2]$$

A parallel process in which Cu + Si react with CH_3Cl, without a Cu_3Si intermediate, cannot be ruled out. For surfaces in which only Cu_2O catalyst was used, reaction (2) might be slower than reaction (1), so that the Cu_3Si phase is larger than the pits and protrudes out of the surface. In contrast, for the Cu/Cu_2O catalyst mixture, reaction (2) might be faster so that even if the amount of Cu_3Si increases as the pits grow, the amount of silicon used up to form methylchlorosilanes is larger, and thus, the pits are partially full.

Catalyst Dispersion

Although the Cu/Cu_2O mixture clearly has better selectivity and activity than either Cu or Cu_2O alone, and a higher Cu fraction yields a more effective catalyst, we have not identified the reason for the differences. Evaporated Cu forms a continuous Cu film on the Si surface, and thus is well dispersed. Even though contact between the Cu and Si is good, and Cu_3Si formed when copper was evaporated onto Si(100) that was held at elevated temperatures, no methylchlorosilanes formed on these surfaces. Copper formate decomposes to form both particles and a Cu film, and the particles appear more active for reaction, even though they are not well dispersed (large Cu–Si contact area). When the particles were brushed off the surface (so that only the Cu film remained) no reaction was observed.

The amount of copper on the Si(100) does not appear to be critical. When 63 mg of Cu powder was used, dmd selectivity was poor and reaction stopped after 10 hr, but when 15 mg of a Cu/Cu_2O mixture was used, good selectivity was obtained. In contrast, when smaller amounts of Cu was used (evaporated Cu or Cu film on brushed sample), no methylchlorosilanes formed. The amounts of copper per cm^2 of Si surface area are larger for the Si(100) surfaces than the values reported in the literature. Lewis *et al.* (33) indicated that copper concentrations of 5–10% are optimal for fluidized bed reactors. These concentrations correspond to 1–15 μg Cu/cm^2 of Si. Ward *et al.* (5) used 9.1 μg Cu/cm^2 Si, and Gaspar-Galvin *et al.* (12) used 37 μg Cu/cm^2 Si. Our lowest amount of copper (90 μg Cu/cm^2 Si) was for evaporated Cu and no reaction was observed. Thus, the amount of copper does not appear to be the limiting factor in the lack of reactivity of evaporated Cu catalyst. Formate solution A resulted in approximately 1 mg Cu/cm^2 and the 82% Cu/18% Cu_2O catalyst had a concentration of 12.3 mg Cu/cm^2. A significant difference between our study and those on powdered silicon in fluidized beds is that Cu that leaves the Si(100) surface (as CuCl, for example) is lost to the reaction, whereas in the fluidized beds it can adsorb on another silicon particle and deposit Cu. Thus, the amount of copper per cm^2 is not a major factor for the different selectivity results between silicon wafers and powdered silicon.

Silicon Oxide Layer

The native oxide layer (2 nm thick) did not appear to inhibit reaction between Cu and Si significantly. When the oxide layer was removed before evaporating Cu onto Si(100), the activity was not improved. Previous studies in which various thickness of Cu were evaporated onto single crystal and polycrystalline surfaces (42, 43) did not show any reaction with CH_3Cl, even though the oxide layer was removed before evaporation for all samples. For the 450-nm Cu layer evaporated at 523 K onto the native oxide layer, Cu_3Si was readily detected by XRD. Even Si(100) surfaces with a 4-nm oxide layer were active when copper formate was used to deposit copper onto them (17). Apparently the interaction between Si and Cu is significantly strong, and the SiO_2 layers are sufficiently nonuniform, that the oxide layer does not significantly inhibit dmd formation. Since the native oxide layer is not removed in the industrial production of dmd, the oxide layer is apparently not a major inhibitor of the reaction.

Copper Formate Catalyst

Lewis *et al.* (16) used various forms of copper formate as catalysts for the direct reaction. They observed significant differences in activity and selectivity for the various formates, which they attributed to the structure of the formate and how it decomposed. They observed that for-

mate decomposes to form Cu, which occurs as both a mirror film and as copper particles. Similarly, others have reported that when dry copper formate decomposes, no Cu_2O forms (27, 28). When our dry copper formate decomposed, it also formed Cu particles (and no Cu_2O), but this Cu was not active for reaction on high purity Si(100). When copper formate from aqueous solution decomposed, however, both Cu and Cu_2O formed, and this catalyst was active for selective formation of dmd. As the formate concentration decreased, the fraction of Cu_2O increased. For a formate solution with concentration in between that of solution A and B, both Cu_2O and Cu phases were detected by XRD in a 1 : 1 ratio and no mirror film was observed. Schuffenecken *et al.* (44) reported that Cu_2O forms from copper formate decomposition in the presence of water, consistent with our observation that for lower formate concentration, the Cu_2O fraction is larger. X-ray analysis of our copper formate after depositing it from solution at 373 K showed that the structure of the copper formate dihydrate had changed, and we could not fit the resulting XRD pattern to any known formate structure. The formate decomposed above 373 K to form an active catalyst. Lewis *et al.* (16) reported that anhydrous formate gave poor selectivity, but a direct comparison to selectivity in our work is difficult since Lewis *et al.* used Zn and Sn promoters, both of which significantly improve selectivity. Zinc also increases Cu–Si interdiffusion rates (45). Lewis *et al.* used technical grade Si (98.4 wt% purity), which can also influence the reaction.

The catalyst formed from copper formate solution A showed good selectivity at short reaction times, but at longer times significant quantities of mdc formed. Indeed, on some samples at long times, mdc became the dominant product (17), in contrast to the industrial reaction, but similar to what has been observed for a fixed bed reactor with high purity Si and CuCl catalyst (12). The main difference between catalysts from formate and from Cu/Cu_2O powder is that a Cu film forms when formate decomposes on the Si surface. This copper film may be responsible for the mdc reaction, but it must *only* be active as a catalyst when Cu or Cu_2O particles are present, since the Cu film was present on the sample after it was brushed, but no products were observed on the brushed surface. Similarly, a copper film formed by evaporating copper was unreactive.

CONCLUSIONS

High-purity single crystal Si(100) surfaces with a native oxide layer serve as excellent models of the reacting silicon surface for the direct synthesis of dimethyldichlorosilane (dmd). The selectivity of the reaction is sensitive to the form of the copper catalyst. A catalyst that contains both metallic Cu and Cu_2O yields a high selectivity for dmd, whereas neither Cu nor Cu_2O alone catalyze this reaction. A Cu_2O catalyst forms a reactive surface for the formation of methyltrichlorosilane, but no dimethyldichlorosilane forms. A 82 wt% Cu/18 wt% Cu_2O powder mixture was found to give the best selectivity for dmd formation. Copper formate was shown to be a good catalyst precursor because it decomposes, when deposited from solution, to form a mixture of Cu and Cu_2O. At longer reaction times, however, selectivity degrades as methyldichlorosilane forms. Formation of Cu_3Si from the interaction of copper metal and silicon is not sufficient to catalyze formation of dimethyldichlorosilane. Many surfaces that form the stoichiometric alloy Cu_3Si are not selective or even reactive for dmd formation, and a correlation was observed between the selectivity for dmd and the orientation of Cu_3Si crystallites on the Si(100) surface. The most selective surfaces had a randomly oriented Cu_3Si phase. The Si(100) surfaces reacted by forming square pyramidal pits that contained Cu_3Si. The sides of the pits were Si(111) planes.

ACKNOWLEDGMENT

We gratefully acknowledge financial support from Elkem Metals Company.

REFERENCES

1. Voorhoeve, R. J. H., "Organohalosilanes: Precursors to Silicones." Elsevier, Amsterdam, 1967.
2. Rochow, E. G., "An Introduction to the Chemistry of the Silicones." Wiley, New York, 1951.
3. McGregor, R. R., "Silicones and Their Uses." McGraw–Hill, New York, 1954.
4. Frank, T. C., and Falconer, J. L., *Langmuir* **1,** 104 (1985).
5. Ward, W. J., Ritzer, A., Carroll, K. M., and Flock, J. W., *J. Catal.* **100,** 240 (1986).
6. Banholzer, W. F., and Burrell, M. C., *J. Catal.* **114,** 259 (1988).
7. Frank, T. C., Kester, K. B., and Falconer, J. L., *J. Catal.* **91,** 44 (1985).
8. Magrini, K. A., Falconer, J. L., and Koel, B. E., "Catalyzed Direct Reactions of Silicon" (K. M. Lewis and D. G. Rethwisch, Eds.), p. 249. Elsevier, New York, 1993.
9. Agarwala, J. P., and Falconer, J. L., *Int. J. Chem. Kinet.* **19,** 519 (1987).
10. Frank, T. C., Kester, K. B., and Falconer, J. L., *J. Catal.* **95,** 396 (1985).
11. Frank, T. C., and Falconer, J. L., *Appl. Surf. Sci.* **14,** 259 (1983).
12. Gaspar-Galvin, L. D., Sevenich, D. M., Friedrich, H. B., and Rethwisch D. G., *J. Catal.* **128,** 468 (1991).
13. Banholzer, W. F., Lewis, N., and Ward, W. J., *J. Catal.* **101,** 405 (1986).
14. Yilmaz, S., Floquet, N., and Falconer, J. L., to be submitted.
15. Lieske, H., Fichtmer, H., Grohmann, I., Selenina, M., Walkow, W., and Zimmerman, R., *in* "Silicon for Chemical Industry" (H. A. Oye and H. Rong, Eds.) p. 16, 1992.
16. Lewis, K. M., Cameron, R. A., and Larnerd, J. M., "Catalyzed Direct Reactions of Silicon" (K. M. Lewis and D. G. Rethwisch, Eds.), p. 117. Elsevier, New York, 1993.

17. Falconer, J. L., and Yilmaz, S., *in* "Silicon for Chemical Industry," Geiranger, Norway (H. A. Oye and H. Rong, Eds.) p. 99, 1992.
18. Kim, J. P., and Rethwisch, D. G., *J. Catal.* **134,** 168 (1992).
19. Davis, L. E., MacDonald, N. C., Palmberg, P. W., Riach, G. E., and Weber, R. E., "Handbook of Auger Electron Spectroscopy," 2nd ed. Physical Electronics, Eden Prairie, MN, 1976.
20. Joint Committee on Powder Diffraction Standards (JCPDS), Standard Powder Diffraction File. International Center for Diffraction Data, Swarthmore, PA.
21. Corn, S. H., Falconer, J. L., and Czanderna, A. W., *J. Vac. Sci. Technol.* **6,** 1012 (1988).
22. Eberhart, J. P., "Structural and Chemical Analysis of Materials," Wiley, p. 203. Wiley, New York, 1991.
23. Viale, D., Weber, G., and Gillot, B., *J. Cryst. Growth* **102,** 269 (1990).
24. Solberg, J. K., *Acta Crystallogr. Sect. A* **34,** 684 (1978).
25. Weber, G., Gillot, B., and Barret, P., *Phys. Status Solidi A* **75,** 567 (1983).
26. Kolster, B. H., Vlughter, J. C., and Voorhoeve, R. J. H., *Recl.* **83,** 737 (1964).
27. Galwey, A. K., Jamieson, D. M., and Brown, M. E., *J. Phys. Chem.* **78,** 2664 (1974).
28. Gunter, J. R., *J. Solid State Chem.* **35,** 43 (1980).
29. Lewis, K. M., McLeod, D., and Kanner, B., *Catalysis* 87 (1988).
30. Suslick, K. S., Cosantante, D. J. and Doktycz, S. J., *Chem. Mater.* **1,** 6 (1989).
31. Sharma, A. K., and Gupta, S. K., *J. Catal.* **93,** 68 (1985).
32. Koerner, G., Schulze, M., and Weis, J., "Silicones: Chemistry and Technology." Vulkan-Verlag, Essen, 1991.
33. Lewis, K. M., and Childres, T. E., U.S. Patent 4,864,044 (1989).
34. Kolster, B. H., *Acta. Crystallogr.* **19,** 1049 (1965).
35. Krylov, V. D., Agafonove, V. I., and Cherenkova, O. I., *Sov. Phys. Crystallogr.* **11,** 699 (1967).
36. Mukherjee, K. P., Bandyopadhyaya, J., Gupta, K. P., *Trans. Metallur. Soc. AIME* **245,** 2335 (1969).
37. Echigoya, J., Enoki, H., Satoh, T., Waki, T., Ohmi, T., Otsuki, M., and Shibata, T., *Appl. Surf. Sci.* **56,** 463 (1992).
38. Chang, C. A., *J. Appl. Phys.* **67,** 566 (1990).
39. Setton, M., Van der Spiegel, J., and Rothman, B., *Appl. Phys. Lett.* **57,** 357 (1990).
40. Harper, J. M. E., Charai, A., Stolt, L., d'Heurle, J. M., and Fryer, P. M., *Mater. Res. Soc. Symp. Proc.* **187,** 107 (1990).
41. Lampe, C., Jansson, U., Harsta, A., and Carlsson, J., *J. Cryst. Growth* **121,** 223 (1992).
42. Magrini, K. A., Falconer, J. L., and Koel, B. E., *J. Phys. Chem.* **93,** 5563 (1989).
43. Magrini, K. A. and Falconer, J. L., "Catalyzed Direct Reactions of Silicon" (K. M. Lewis and D. G. Rethwisch, Eds.), p. 265. Elsevier, New York, 1993.
44. Schuffenecker, R., Trambouze, Y., and Prettre, M., *Ann. Chim.* **7,** 133 (1962).
45. Potochnik, S. J. and Falconer, J. L., *J. Catal.* **147,** 101 (1994).